ILLINOIS INSTITUTE OF TECHNOLOGY

Gasification Transport: A Multiphase CFD Approach and Measurements

DE-FG26-06NT42736

Dr. Veeraya Jiradilok

&

Dimitri Gidaspow

Distinguished University Professor

Chemical Engineering and Environmental Department
Illinois Institute of Technology
Chicago, IL 60616

June 5, 2007

OUTLINE

- Introduction
- Computation of gas and solid dispersion coefficients in turbulent risers and bubbling beds
- Computation of turbulence and dispersion of cork in the NETL riser
- Experiment of dispersion of FCC particles in the 2D IIT riser
- Gasifier fuel cell

PART 1

Introduction

Fluidization Flow Regime Computations

ILLINOIS INSTITUTE OF TECHNOLOGY
Transforming Lives. Inventing the Future.

BATCH

CONTINUOUS

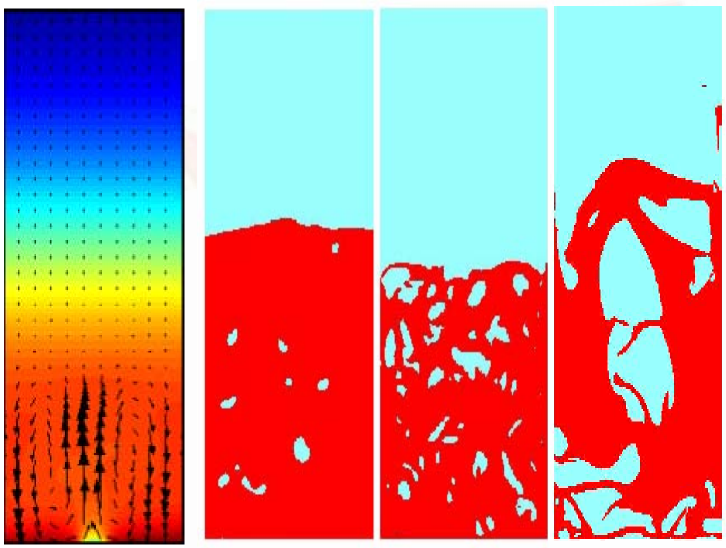

Nano **Group C** **Group A** **Group B**

For Bubbling
U_{mf} > 0.1 random oscillation velocity
No bubbles for 10 nm particles

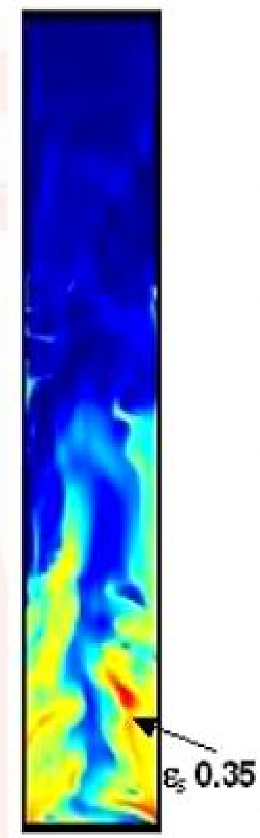

Cluster

$\varepsilon_s \approx 0.4$

$\varepsilon_s \approx 0.14$

$\varepsilon_s \approx 0.03$

Snake-like Oscillation

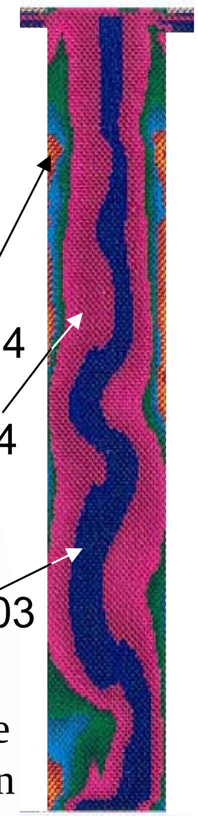

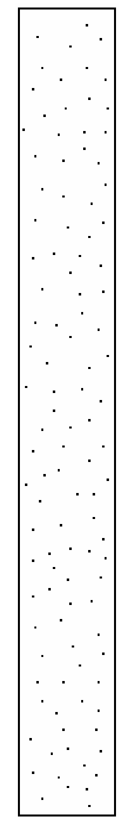

Nanoparticle Flow	Bubbling Bed	Turbulent Fluidization	Fast Fluidization	Dense Suspension Flow	Pneumatic Transport
Jung &Gidaspow, 2002	Gelderbloom et al, 2003	Jiradilok et al , 2006	Tsuo & Gidaspow, 1990 Neri & Gidaspow, 2000 Gidaspow & Mostofi, 2003	Sun & Gidaspow,1999	

Increasing Gas Velocity

INTRODUCTION

Traditional design of gasifiers for the FutureGen project requires the knowledge of dispersion coefficients. However they are known to vary by 5 orders of magnitudes.

From experimental investigations, the dispersion coefficients are known to be large for large diameter bubbling beds and small at low gas velocities. Surprisingly they differ by two to three orders of magnitudes at the same gas velocity.

This study presents a computational method of determining the gas and solid axial and radial dispersion coefficients.

INTRODUCTION

The physical definition of dispersion coefficients is based on the kinetic theory of gases. For diffusion of gases or particles, the diffusivity is defined as the mean free path times the average velocity.

$$D = L \times \overline{C}$$

The mean free path is obtained from the average velocity and collision time.

$$L = \overline{C} \times \tau$$

Therefore, the dispersion matrix can be defined as the Reynolds stresses times the collision time.

$$D_P = \overline{CC} \times \tau$$

TURBULENT DISPERSION COEFFICIENTS

Turbulent dispersion coefficients can be obtained as a function of normal Reynolds stress and the Lagrangian integral time scale as described below.

$$\boxed{D_{Turbulent}(a) = \overline{v'(a)v'(a)}T_L}$$

= Turbulent Kinetic energy × Characteristic Time

where, $\overline{v'(a)v'(a)}$ Reynolds normal stress in a direction

$$T_L = \int_0^{\infty} \frac{\overline{v'(t)v'(t+t')}}{\overline{v'^2}} dt'$$

Lagrangian integral time scale

$$T_L \approx T_E$$

Lagrangian integral time scale approximately equals Eulerian integral time scale

PART 2

Computation of gas and solid dispersion coefficients in turbulent risers and bubbling beds

Turbulent riser Bubbling beds

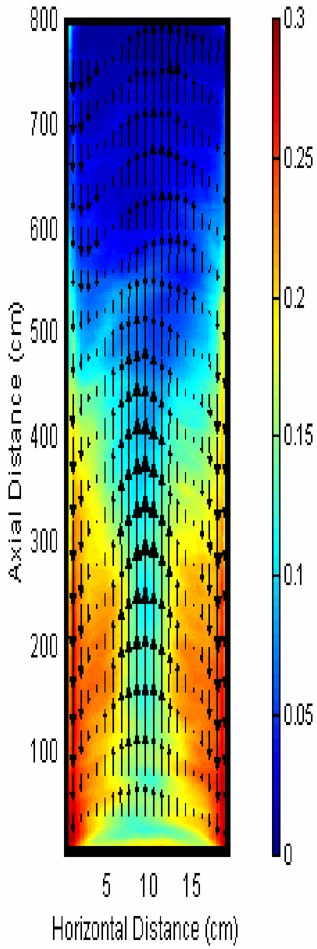

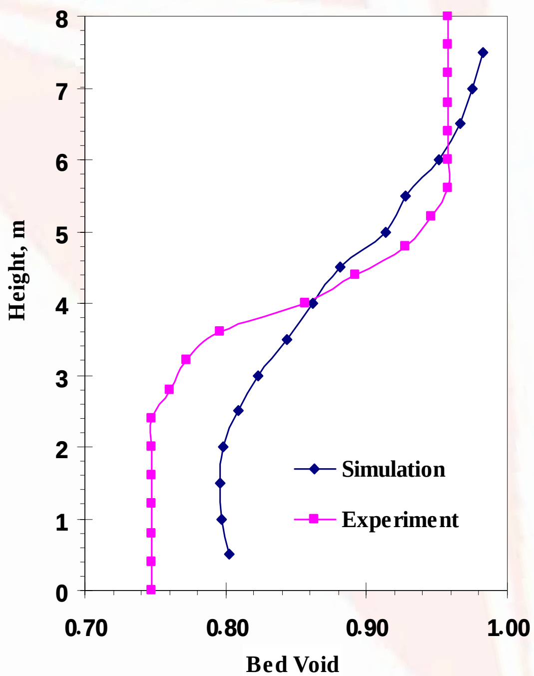

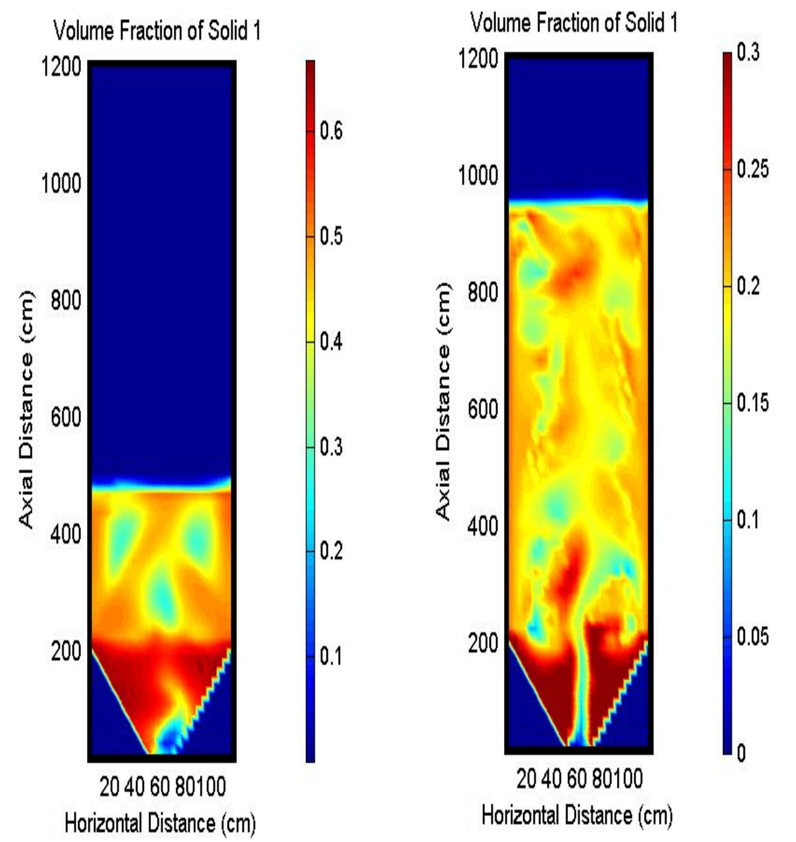

(a) 1 atm (b) 25 atm

Typical time series of hydrodynamic velocities (*v*)

for particles in the center region at a bed height of 4 m at 25 atmospheres.

Axial Direction

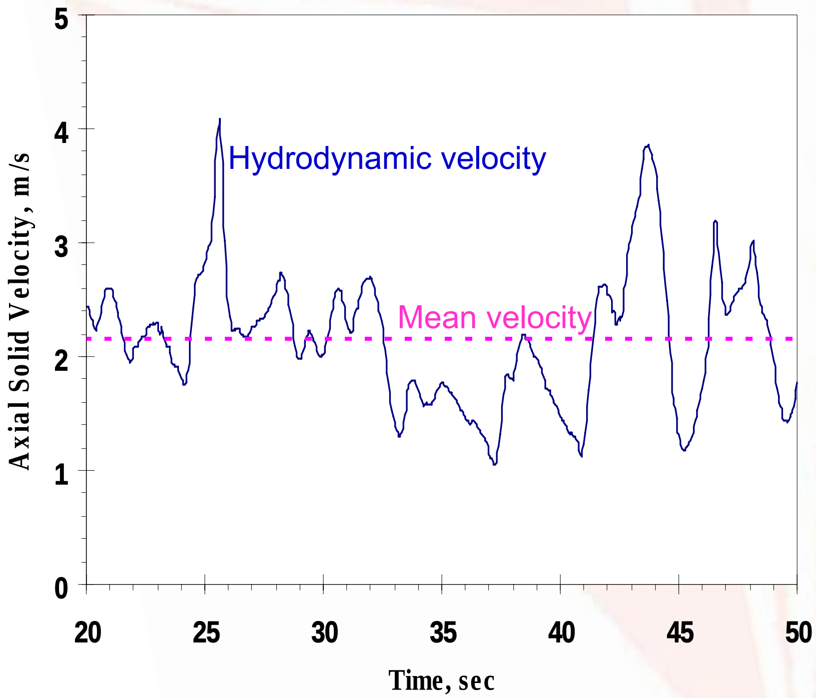

Radial Direction

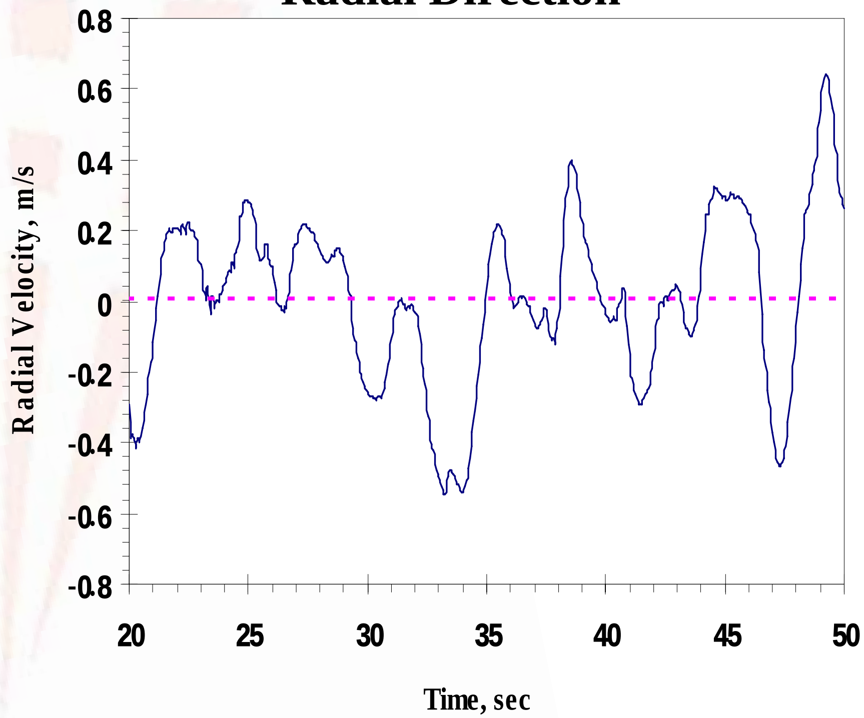

$$\bar{v}_i(r) = \frac{1}{m}\sum_{k=1}^{m} v_{ik}(r,t)$$

$$< V_i V_i > (r) = \frac{1}{m}\sum_{k=1}^{m}(v_{ik}(r,t) - \bar{v}_i(r))(v_{ik}(r,t) - \bar{v}_i(r))$$ Reynolds stress per bulk density

ILLINOIS INSTITUTE OF TECHNOLOGY
Transforming Lives. Inventing the Future.

Normal Reynolds stress per bulk density of gas and solid phases at 6 m.

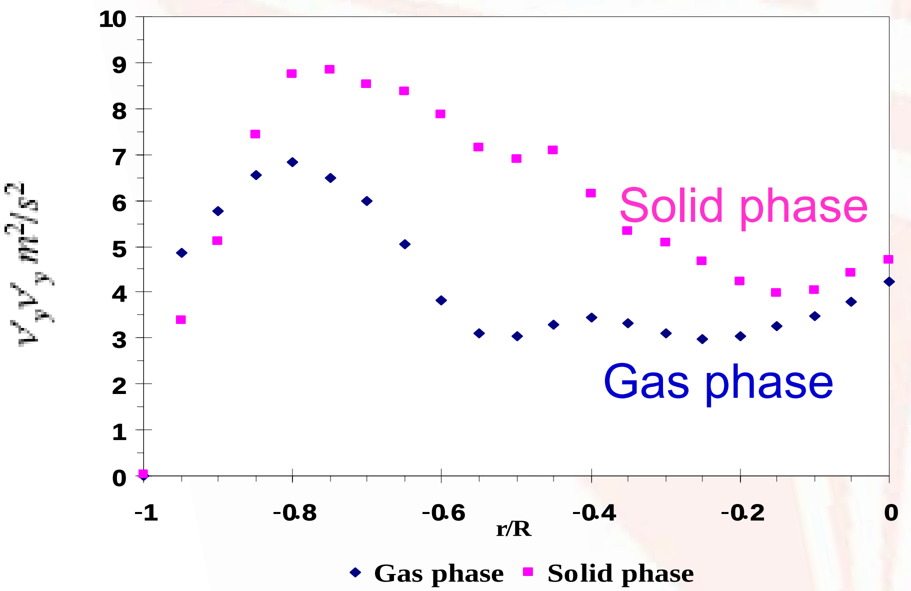

Axial Direction

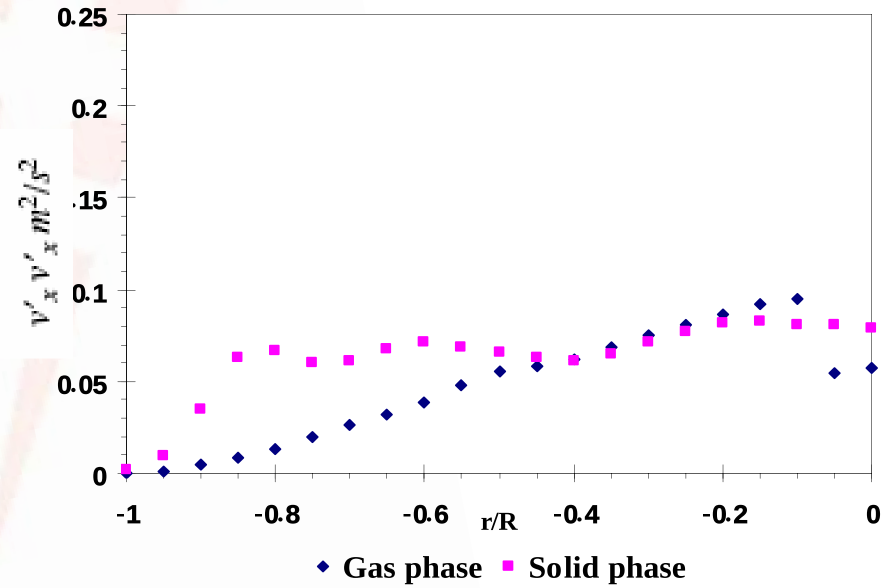

Radial Direction

Typical autocorrelation functions of solid phase

for Ws = 98.8 kg/m2-s and Ug = 3.25 m/s

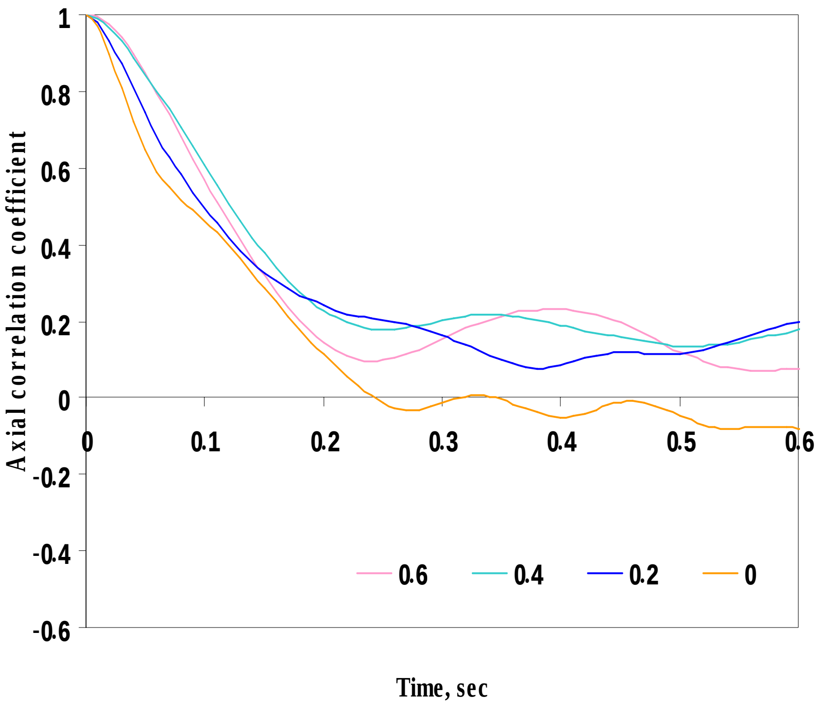

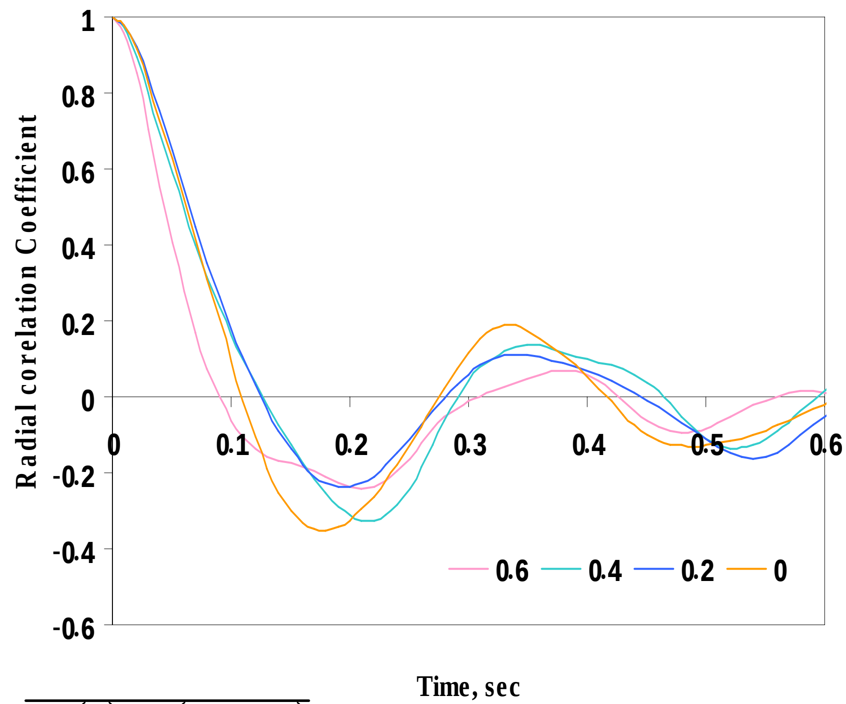

Autocorrelation functions

$$R_E(\vec{a}, t') = \frac{\overline{v'(t)v'(t+t')}}{\overline{v'^2}}$$

Eulerian integral time scale

$$T_E = \int_0^\infty R_E(\vec{a}, t')dt' = \int_0^\infty \frac{\overline{v'(t)v'(t+t')}}{\overline{v'^2}} dt'$$

Effect of the bed diameter on experimental and computed solids dispersion coefficients

for bubbling and turbulent fluidized beds for Geldart A and B particles

$$D_{Turbulent}(a) = \overline{v'(a)v'(a)}T_L$$ = Turbulent Kinetic energy × Characteristic Time

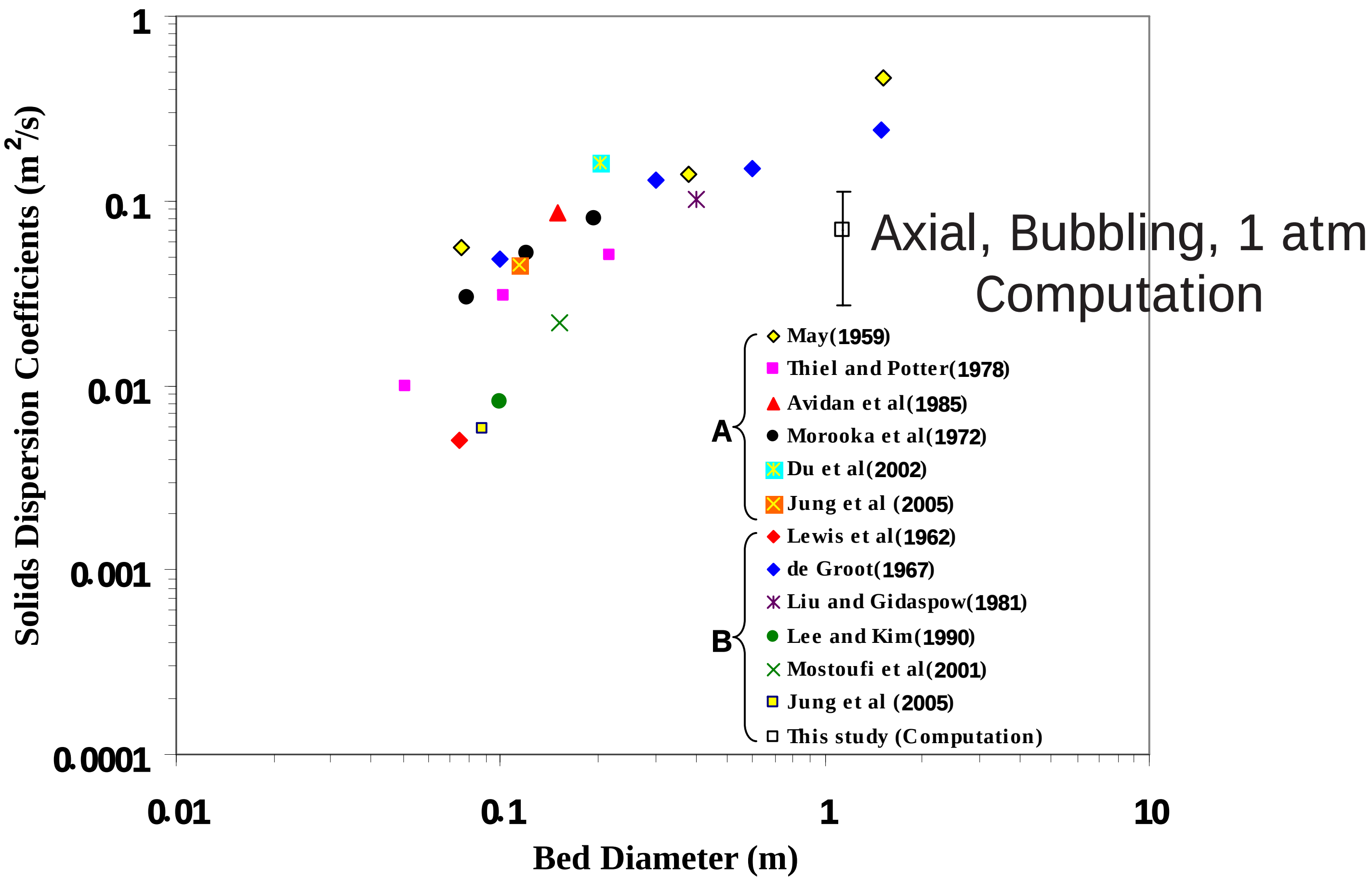

Effect of the gas velocity on experimental and computed gas dispersion coefficients

Axial Direction

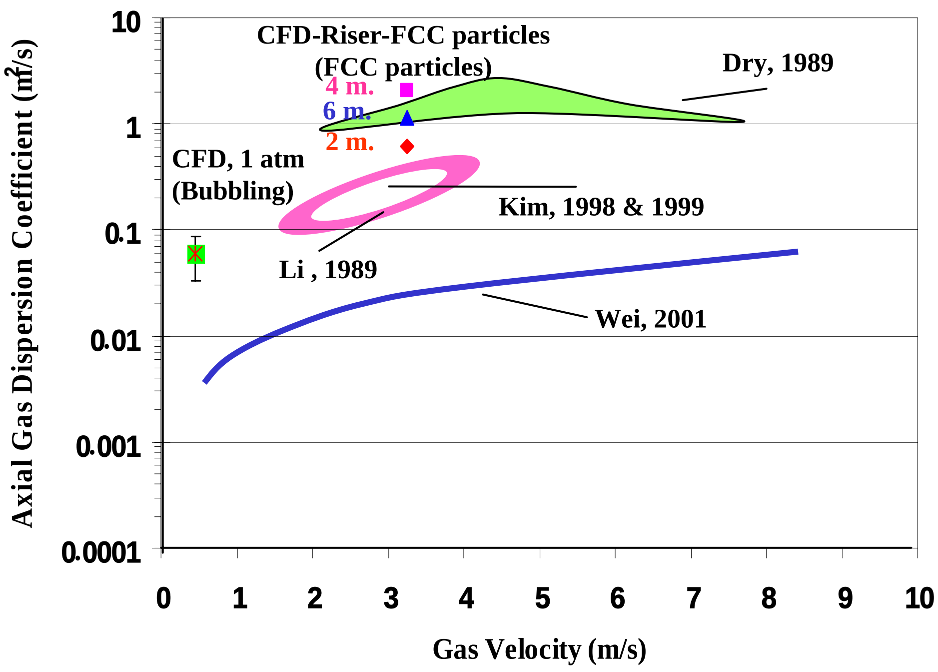

Radial Direction

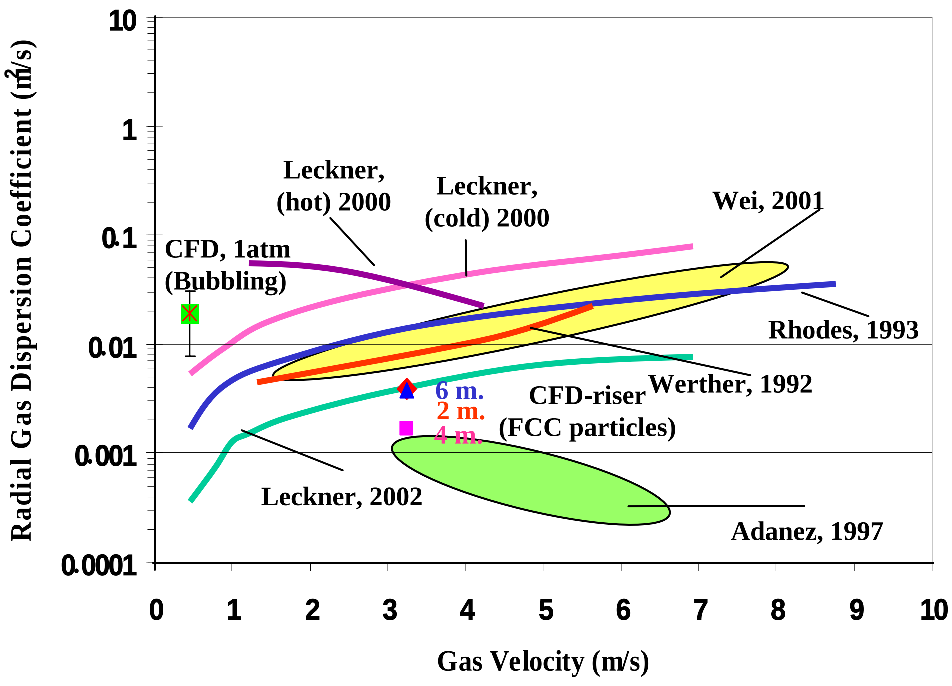

Axial solids dispersion coefficients

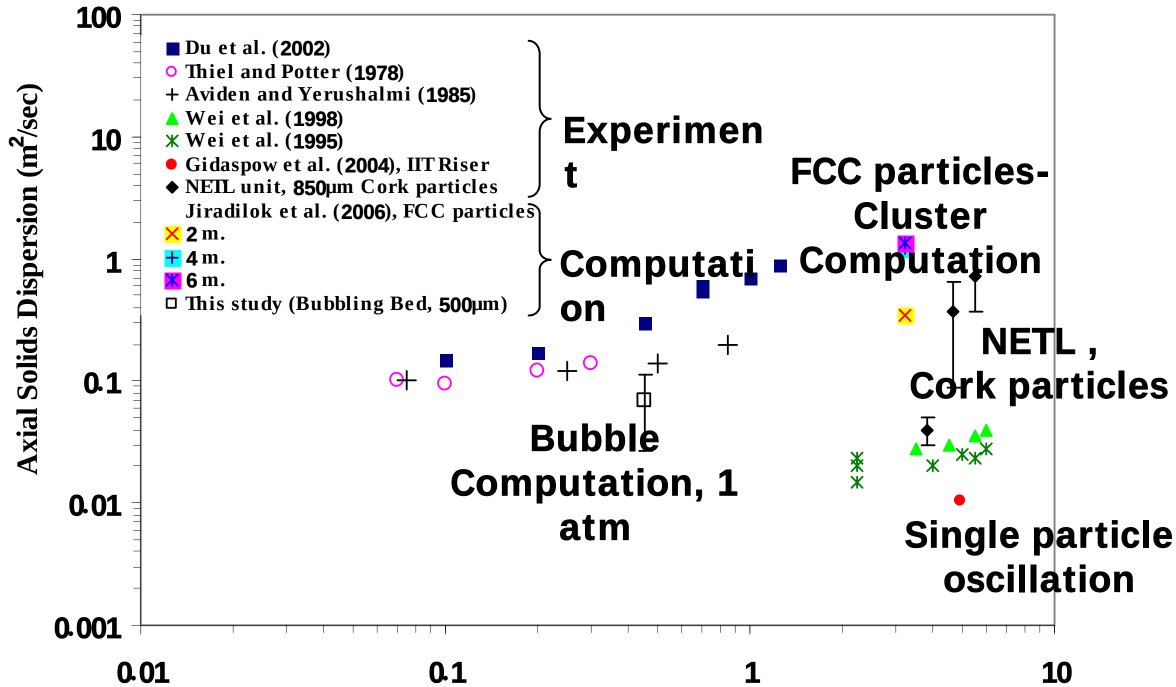

Radial solids dispersion coefficients

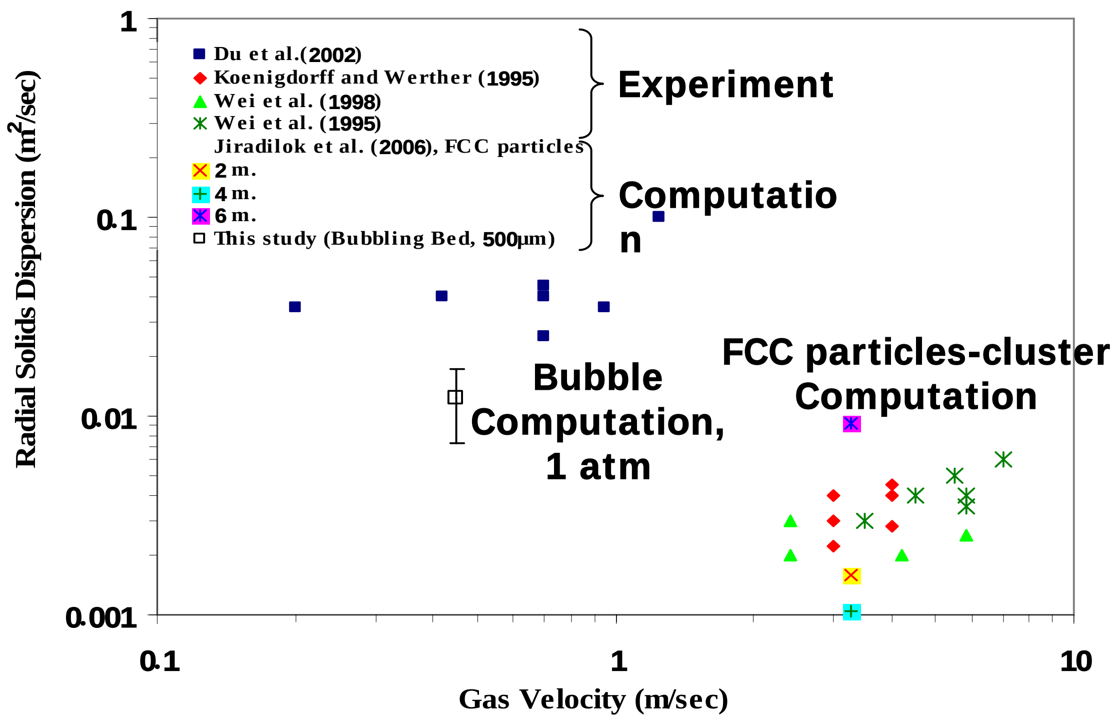

PART 3

Computation of turbulence and dispersion of cork in the NETL riser

DOE NETL CFB UNIT

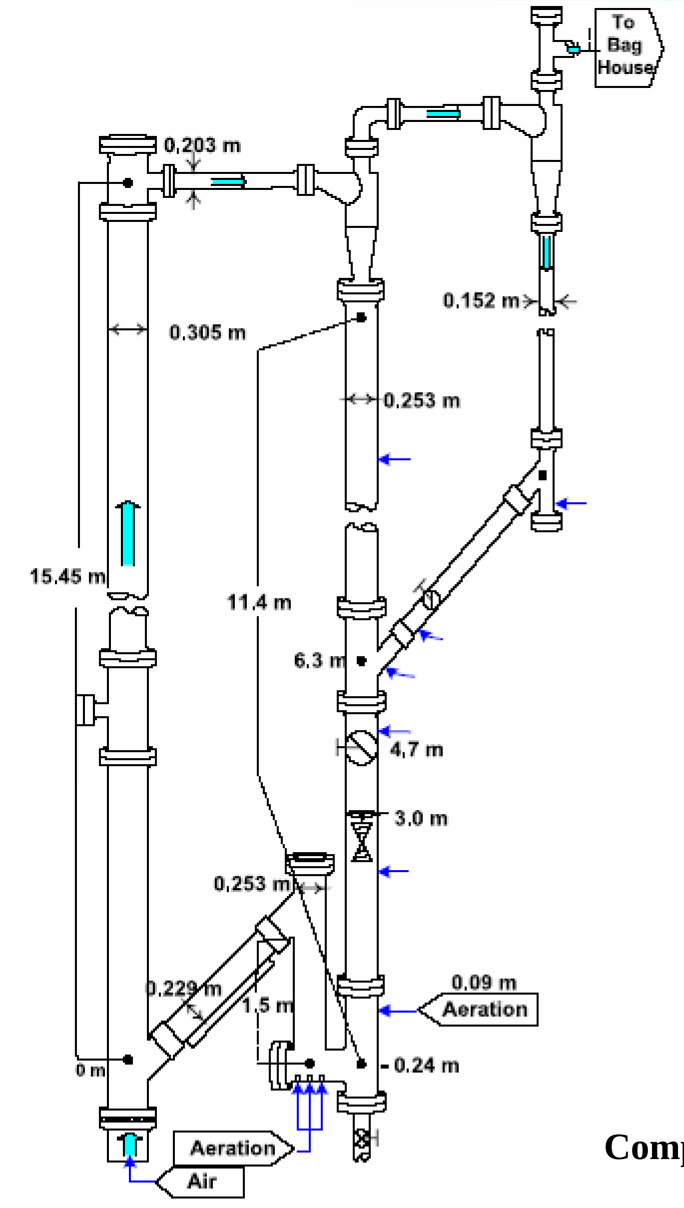

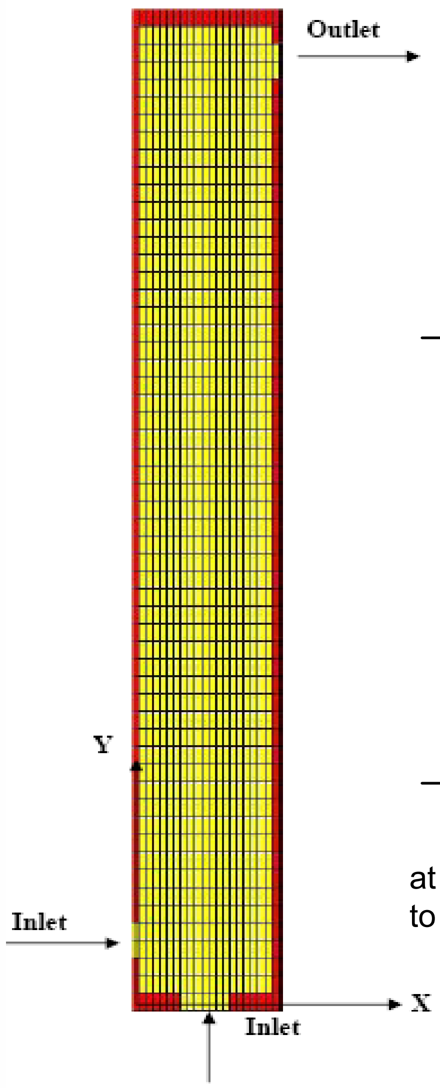

Computational domain of riser section of a CFB NETL unit

Cork characteristics

Particle density	189	kg/m^3
Bulk density	95	kg/m^3
Particle diameter	812	micron
Terminal velocity	0.86	m/s
Minimum fluidization velocity	0.07	m/s
Packed bed voidage	0.49	

Cork is an excellent bed material when tested at ambient conditions in air yields a similar density to that of coal converted to 10-20 atm and 1000^{o}C

A comparison of computational solid volume fraction profiles of cork particles to the NETL Morgantown riser data for three solids fluxes.

Ug 4.71 m/s

a) Ws 3.46 kg/m2.s b) Ws 10.37 kg/m2.s c) Ws 17.1 kg/m2.s

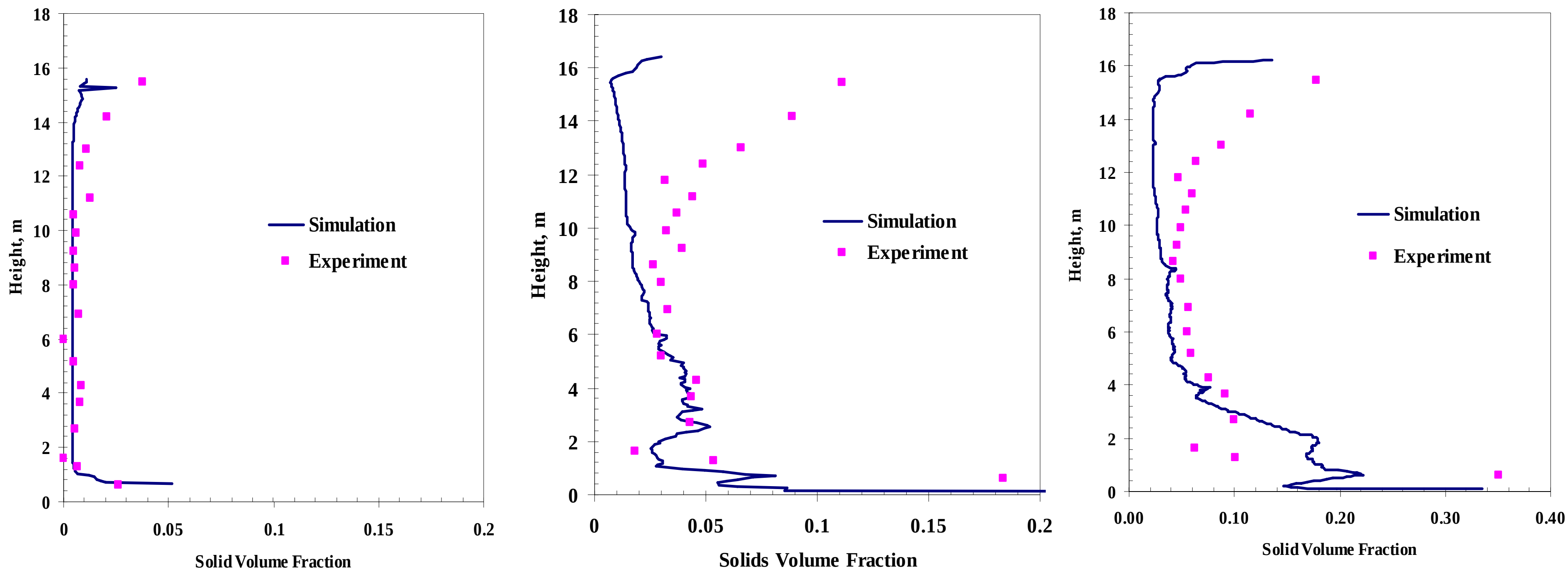

- In the experiment, the solids volume fraction profiles were obtained from the differential pressure drop. $\frac{d\Delta P}{dz} = \rho_s \varepsilon_s g$
- There is a reasonable agreement between the experiment and the simulation results, especially at the low flux.
- At higher solid fluxes the simulated solids volume fractions are close to the experimental measurements, but deviate significantly at the top of the riser.
- This disagreement may be due to use of simplified geometry in the simulation and over-prediction of the experimental volume fractions

Instantaneous solid volume fraction flow structure for two solids fluxes.

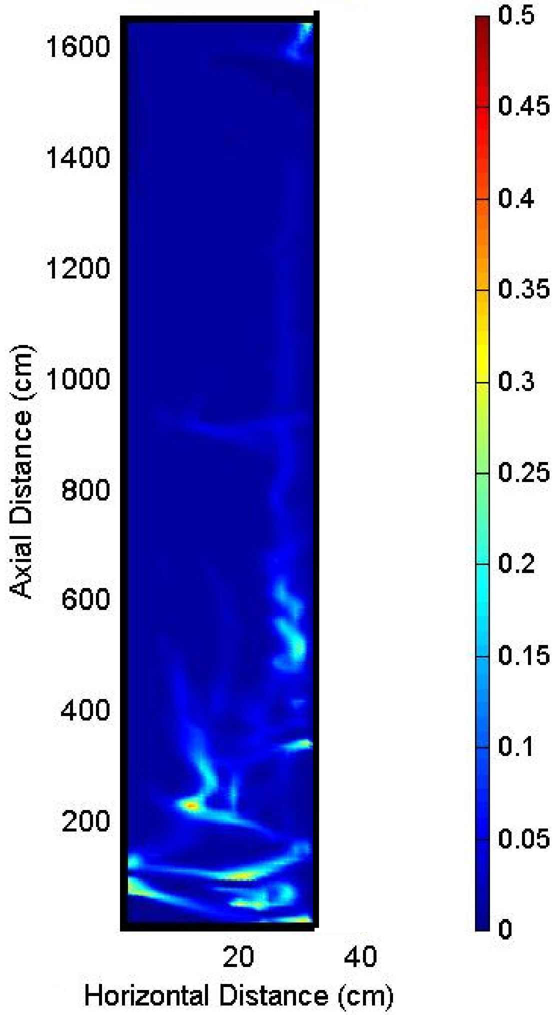

a) Ws 10.37 kg/m^2.s & Ug 4.71

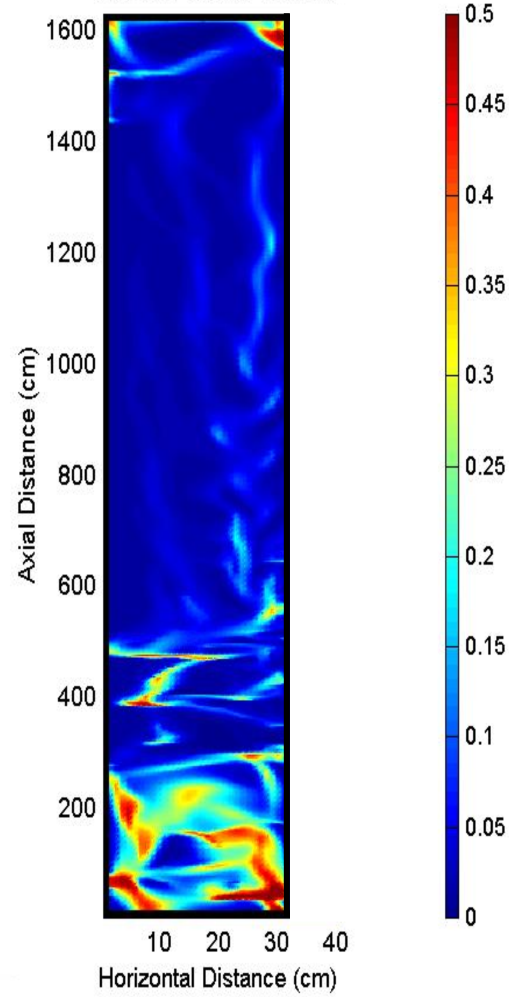

b) Ws 17.1 kg/m^2.s & Ug 4.71 m/s

For high flux, cluster formation occurs, especially at the bottom of the riser.

Axial profile of laminar granular temperature

averaged across the riser. **at the wall the riser.**

Ws = 10.37 kg/m².s Ug = 4.71 m/s

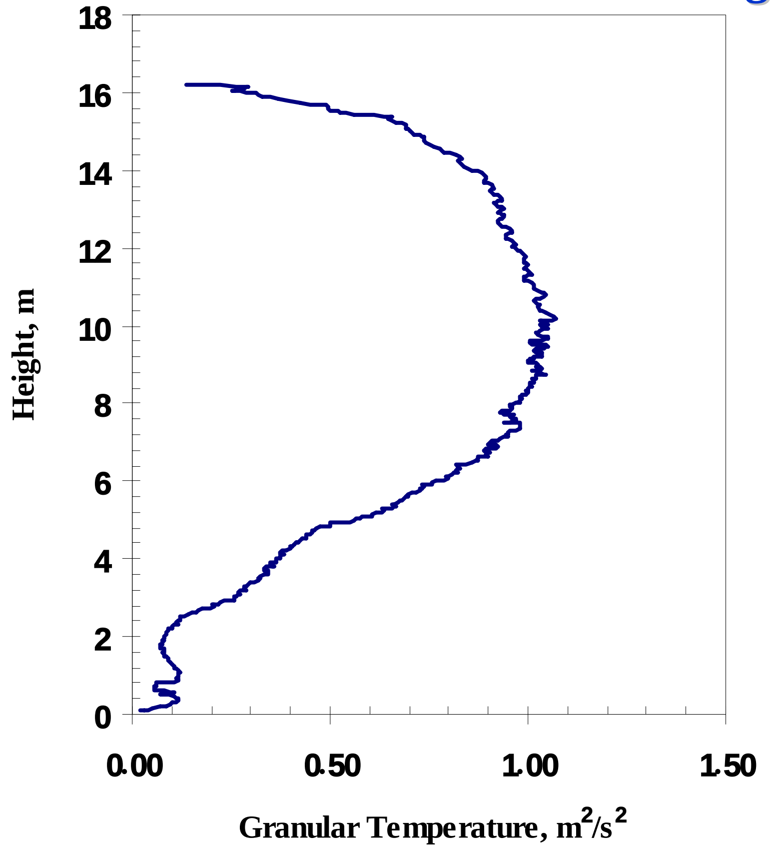

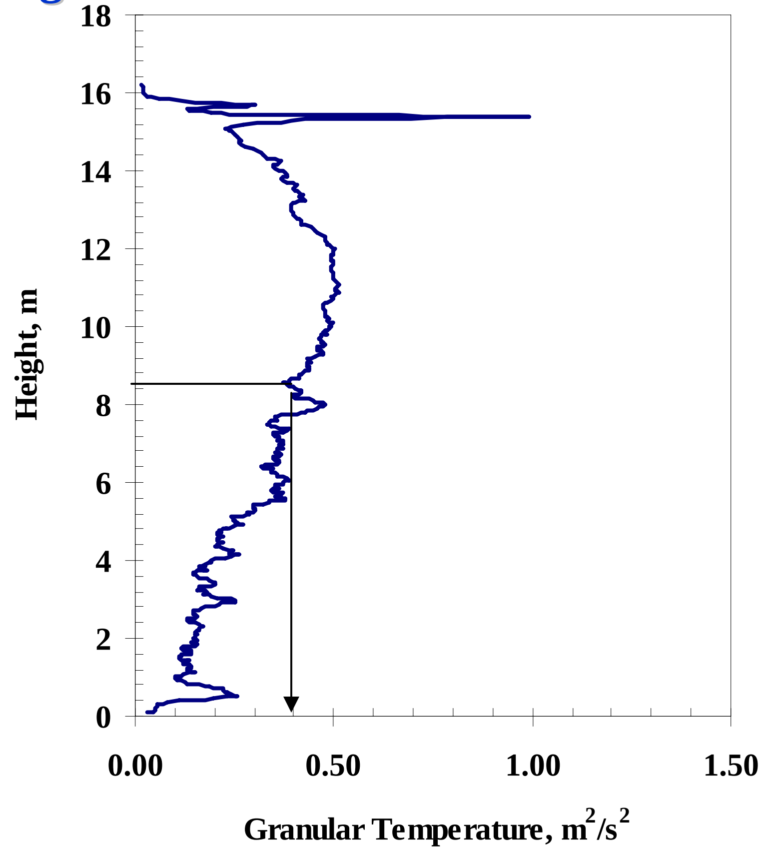

• The granular temperature is ranged form about 0.4 to 0.9 m^2/s^2. There is a reasonable agreement between the experiment of Breault et al. (2005) and the simulation results.

Computed radial and axial gas and solids Reynolds stresses for Ws = 10.37 kg/m².s Ug = 4.71 m/s

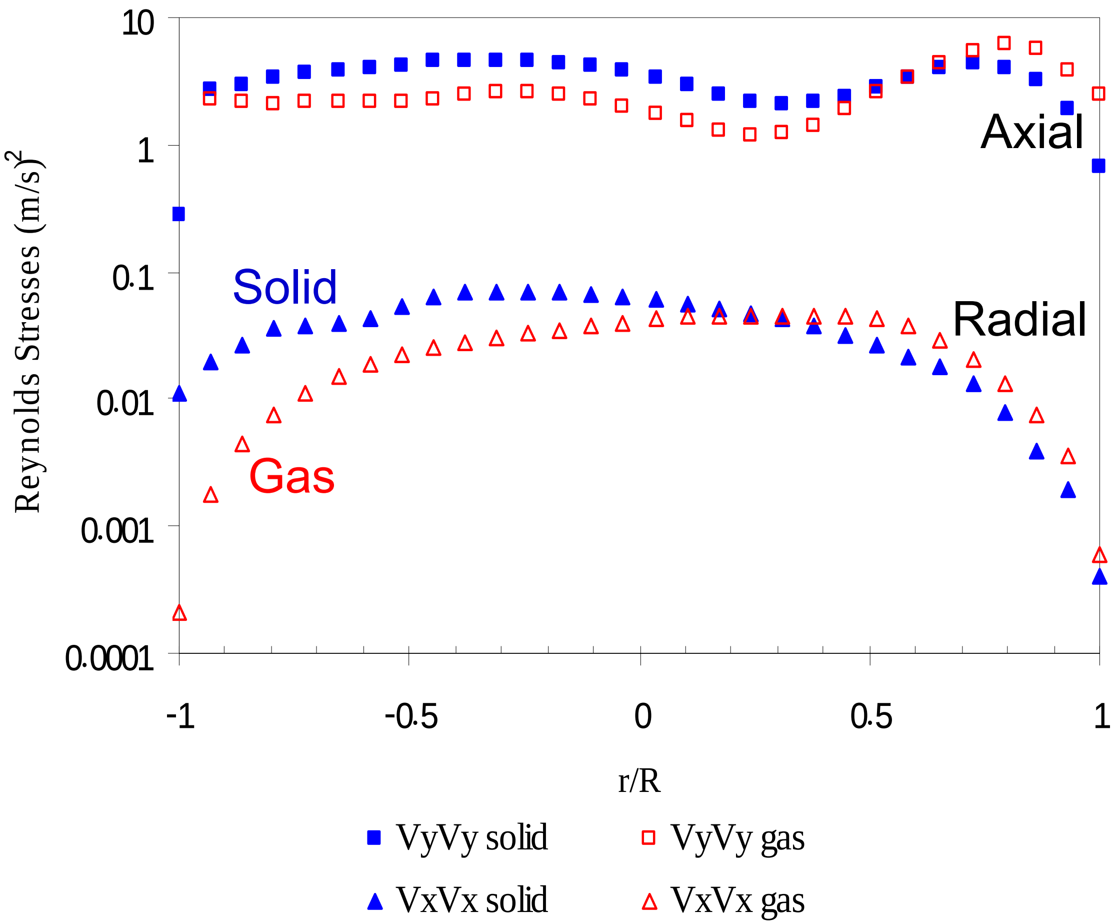

The mean velocity particle

$$\bar{v}_i(r) = \frac{1}{m}\sum_{k=1}^{m} v_{ik}(r,t)$$

The normal Reynolds stress

$$\overline{v_i' v_i'} = \frac{1}{m}\sum_{k=1}^{m}\left(v_{ik}(r,t) - \bar{v}_i(r)\right)\left(v_{ik}(r,t) - \bar{v}_i(r)\right)$$

- The Reynolds stresses use to calculate the turbulent properties such as turbulent granular temperature, energy spectrum, etc.
- They can be calculated as a function of hydrodynamic velocity and mean velocity.
- The computations show that the gas and the solids Reynolds stresses are close to each other.
- The anisotropic characteristics of the particle and gas fluctuations are clearly shown.
- The axial Reynolds stresses are larger than the radial ones due to their production by the large gradient of axial velocity.

A comparison of vertical and horizontal wall region energy spectra for Ws = 3.46 kg/m^2.s Ug = 4.71 m/s

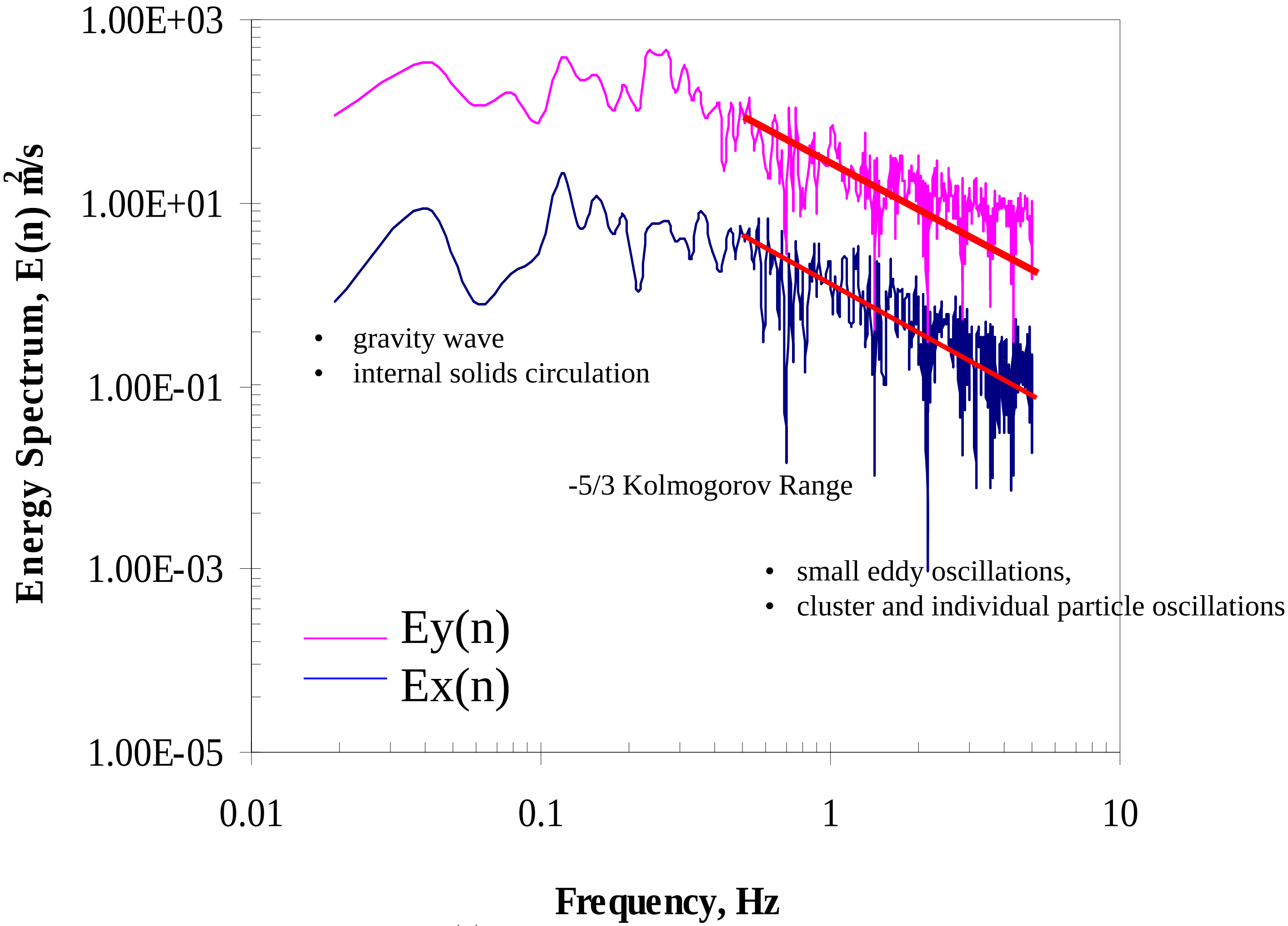

We can estimate the energy spectrum, $E_y(n)$, from the Fourier transforms of $v'_y v'_y$ using the fast Fourier transform (FFT) technique.

A theoretically based correlation of particulate viscosity for cork particles using simulation data

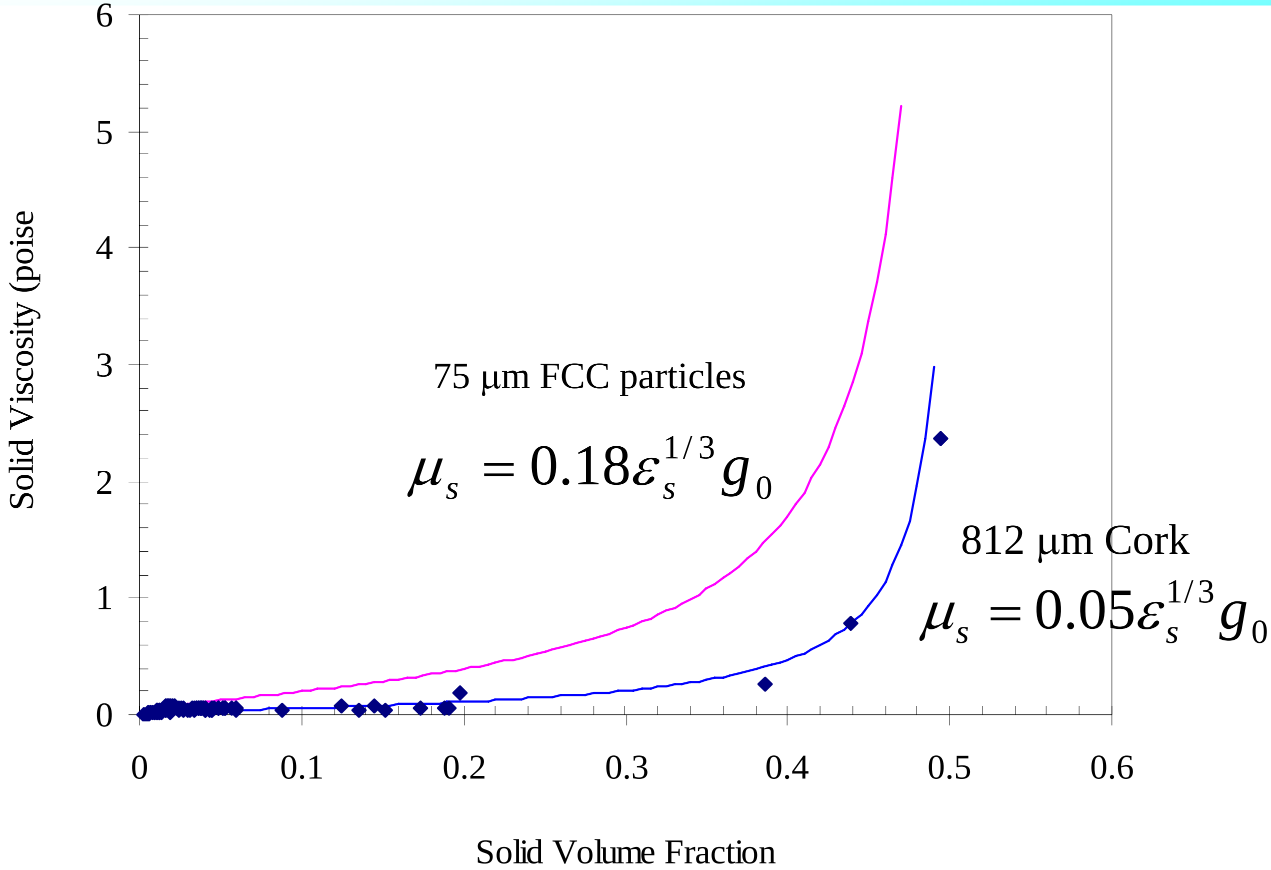

- One of the transport coefficients is the solid viscosity. In the kinetic theory model, the solids viscosity is a function of granular temperature.
- Figure shows the computed solids viscosity as a function of solid concentration.
- The solid viscosity increases with increasing the solid concentration.
- An empirical correlation was corrected for the lower particle density and higher particle diameter to give the correlation for 812 micron cork particles,

A comparison of computed to measured dispersion coefficients for three solids fluxes at a gas velocity of 4.71 m/s

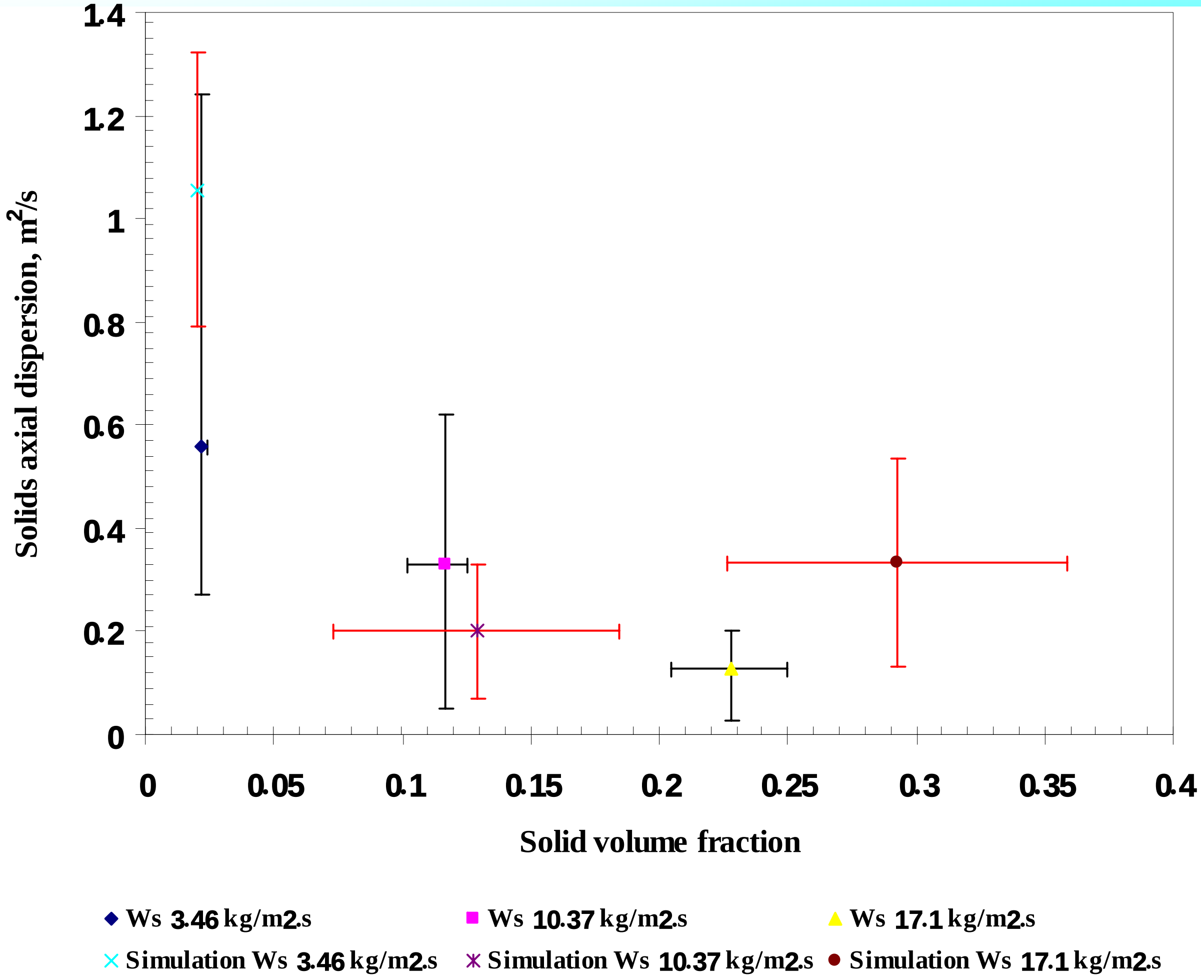

•The solids dispersion coefficients decrease with increasing the apparent solid volume fraction.

A comparison of computed to measured dispersion coefficients for two gas velocities at the solid flux of 10.37 kg/m^2.s

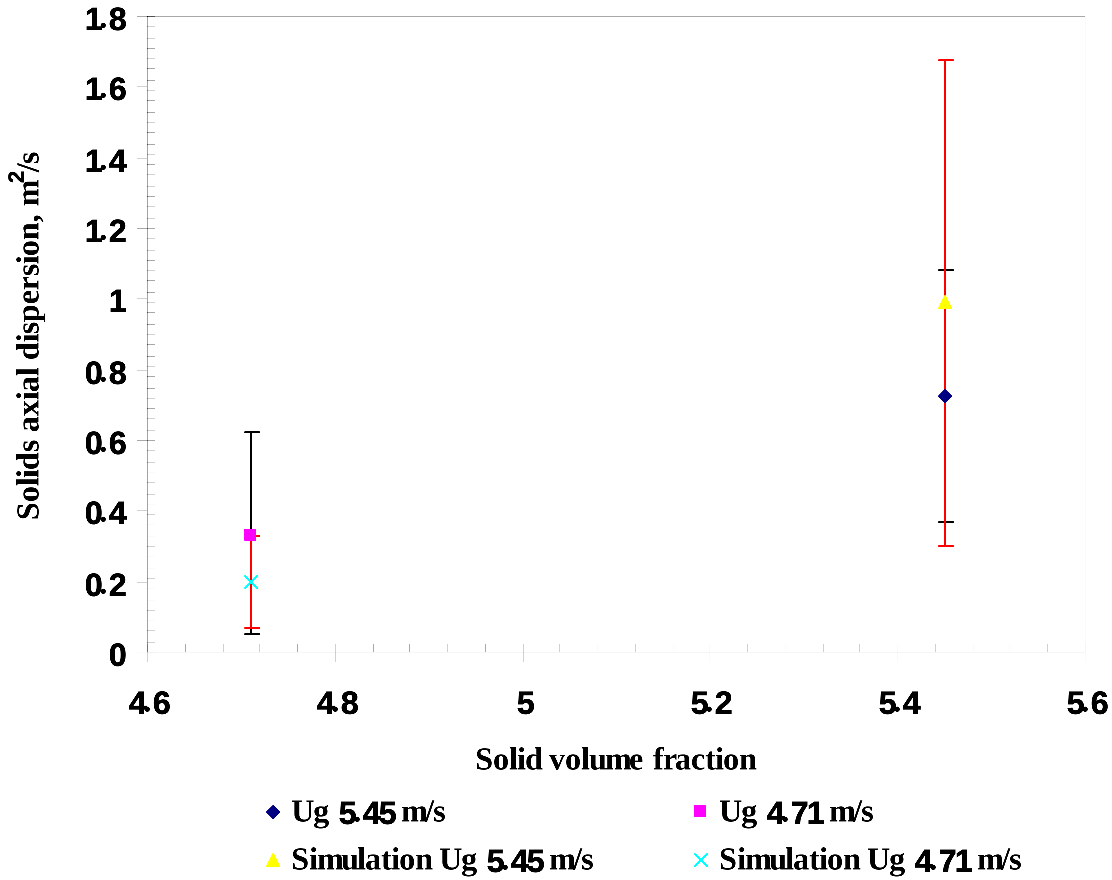

- The solids dispersions are increasing with an increase of gas velocity due to large oscillations at higher gas velocities.

AXIAL AND RADIAL DISPERSION COEFFICIENTS OF GAS PHASE

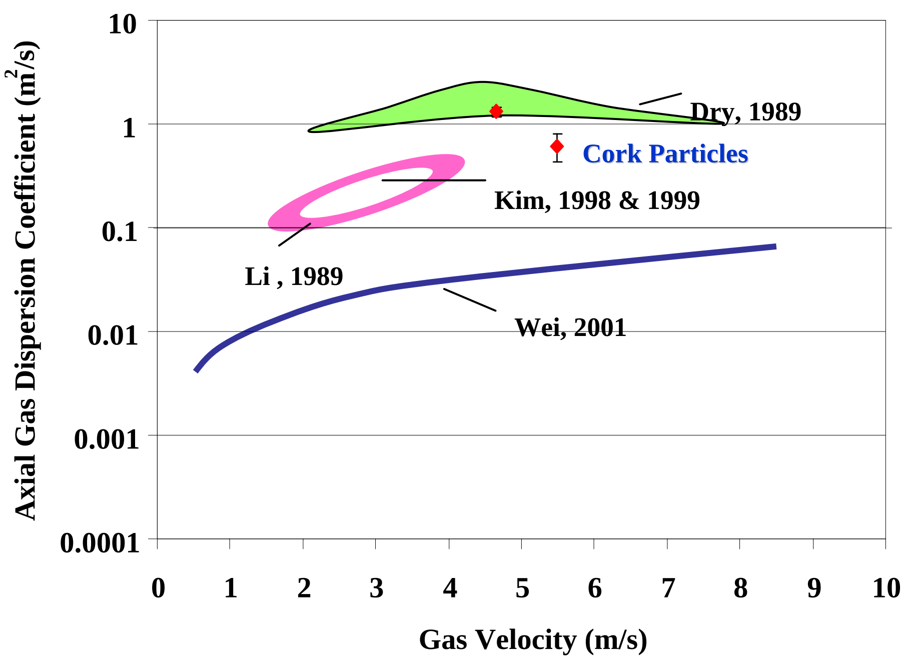

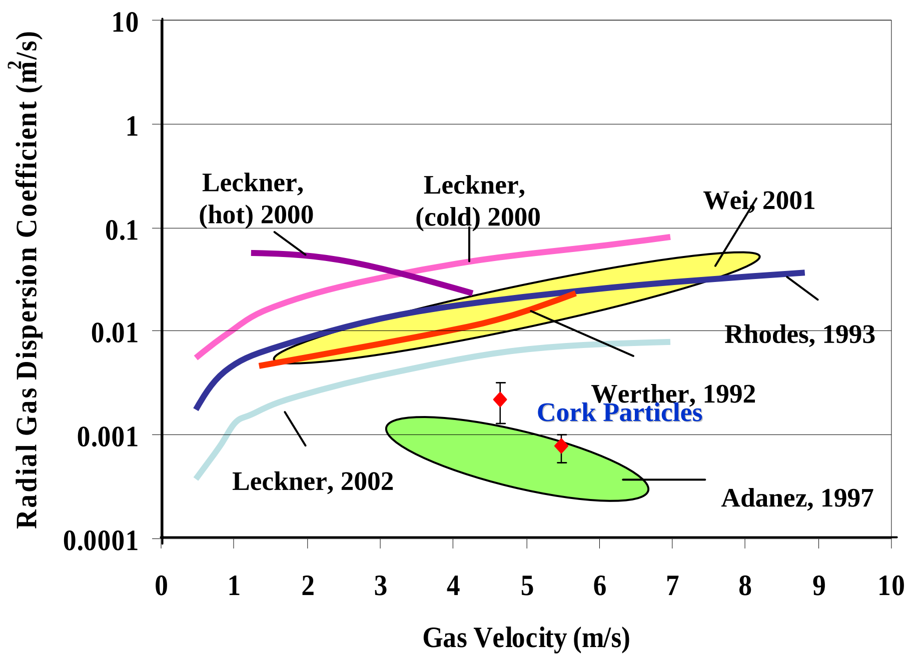

- Figures show the comparisons of computed axial and radial gas dispersion coefficients with the literature survey by Breault (2006).
- The computed dispersion coefficients are in the range of the literature data.

Breault R.W., A review of gas–solid dispersion and mass transfer coefficient correlations in circulating fluidized beds. Powder Technology 163(1-2), (2006) 9-17.

Comparisons between computed solid dispersion coefficients and the literature survey for both directions , axial and radial

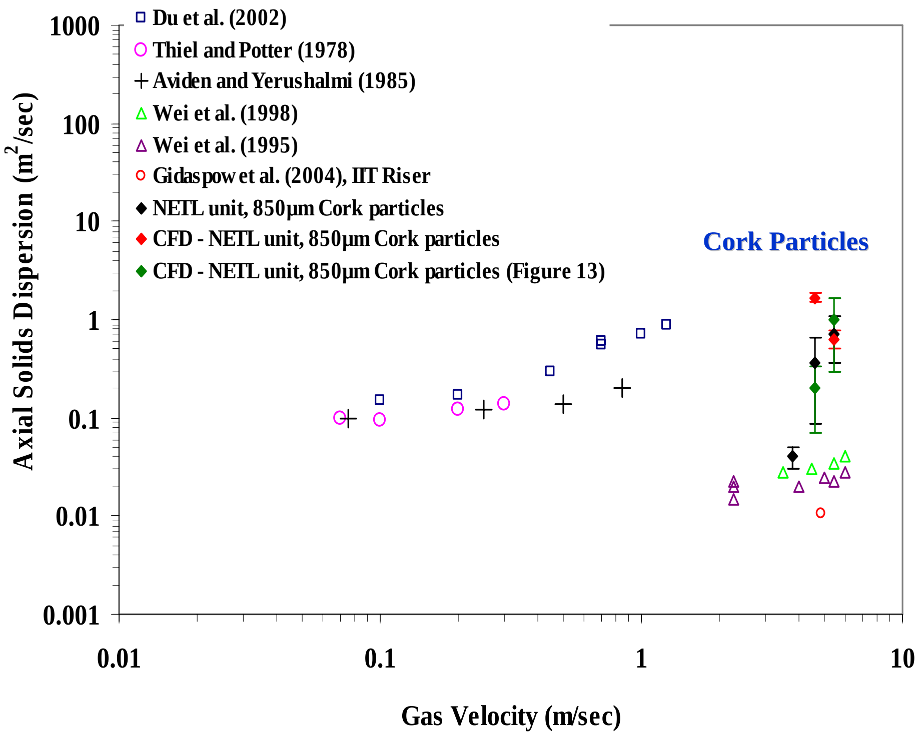

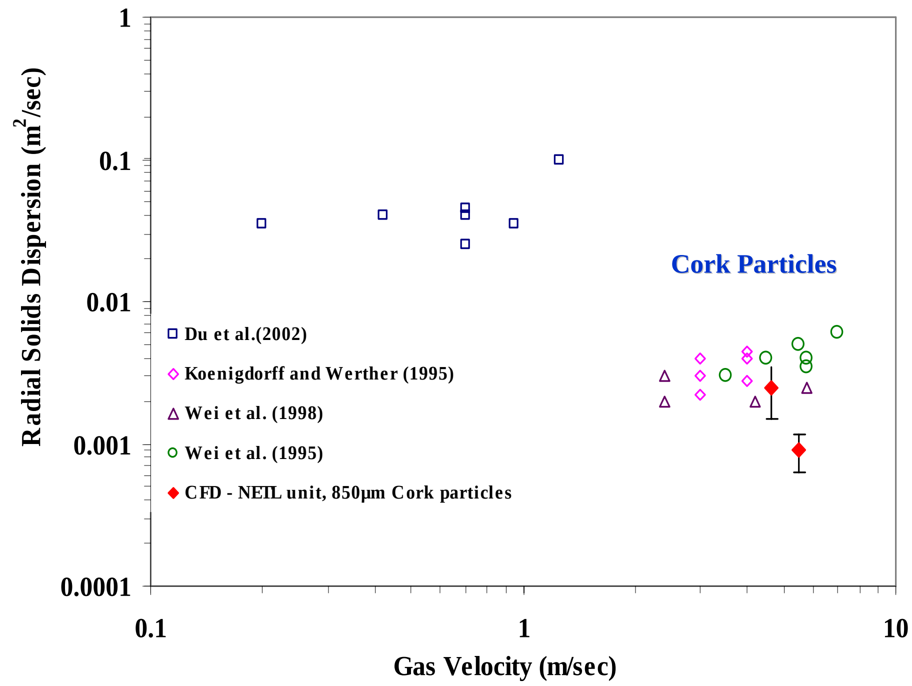

- The computations show that the solids dispersion coefficients are in the range of the literature data.
- The radial dispersion coefficients in the riser are two to three orders of magnitude lower that the axial dispersion coefficients.

PART 4

Experiment of dispersion of FCC particles in the 2D IIT riser

Experimental Setup

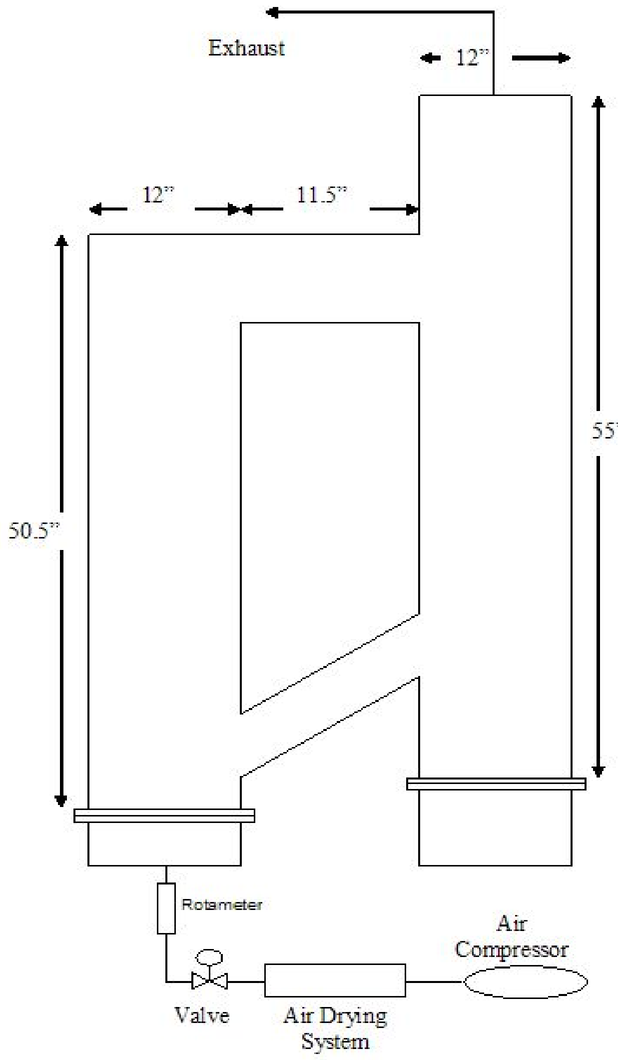

IIT 2-dimensional circulating fluidized bed

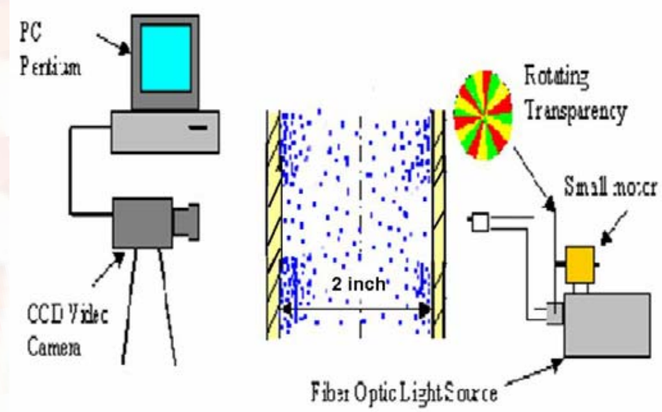

Particle image velocity measurement system

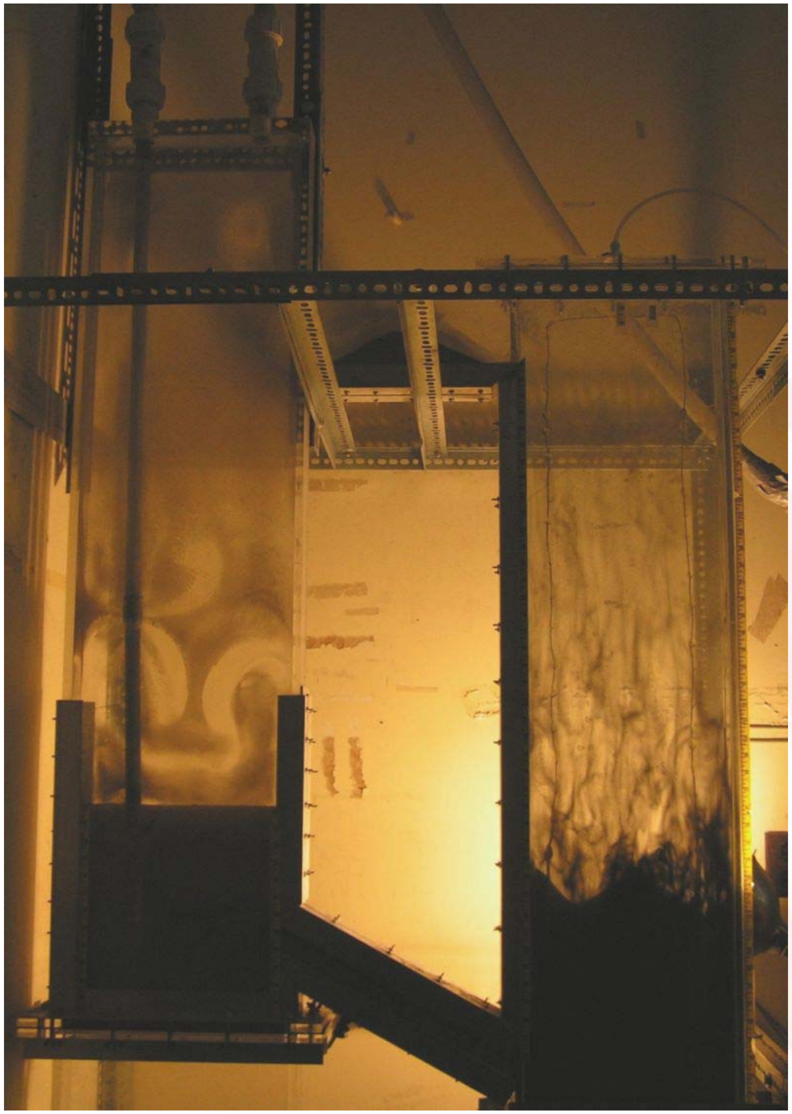

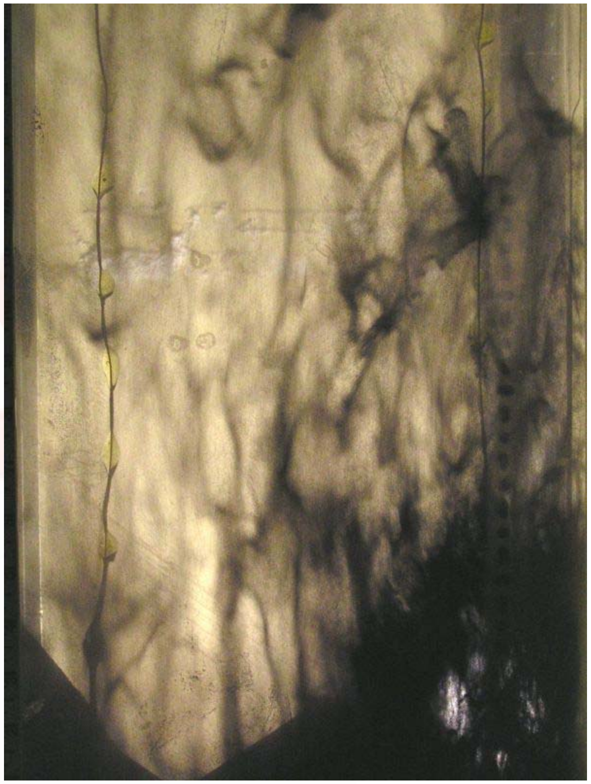

2-Dimensional circulating fluidized bed showing clusters formed by 75 µm FCC particles

Instantaneous Velocities

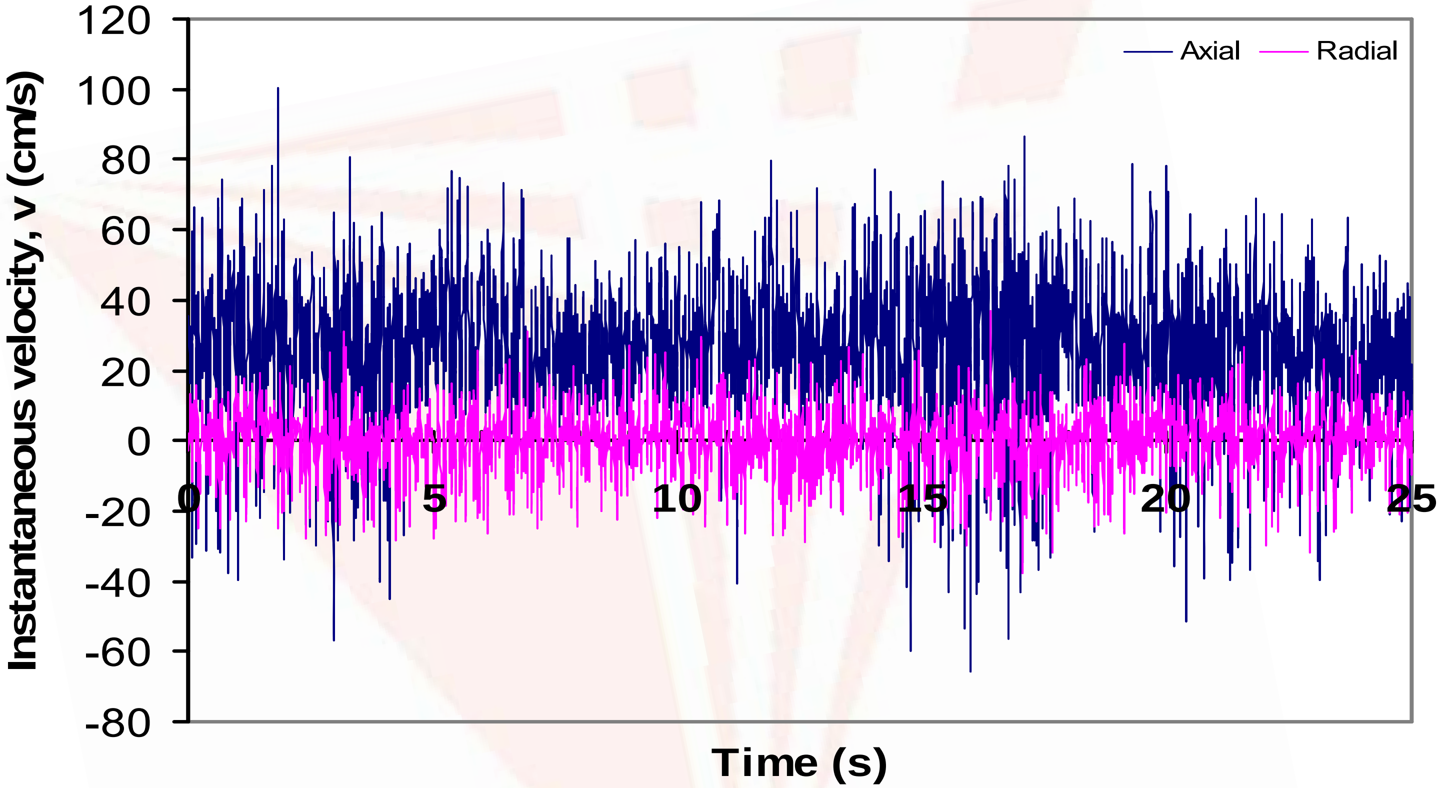

Oscillation of instantaneous velocity in radial and axial directions obtained by CCD camera technique at a measuring height 69.85 cm

$$(\overline{c_r} = 0.06 cm/s \,,\quad \overline{c_a} = 23.21 cm/s \,)$$

Hydrodynamic Velocities

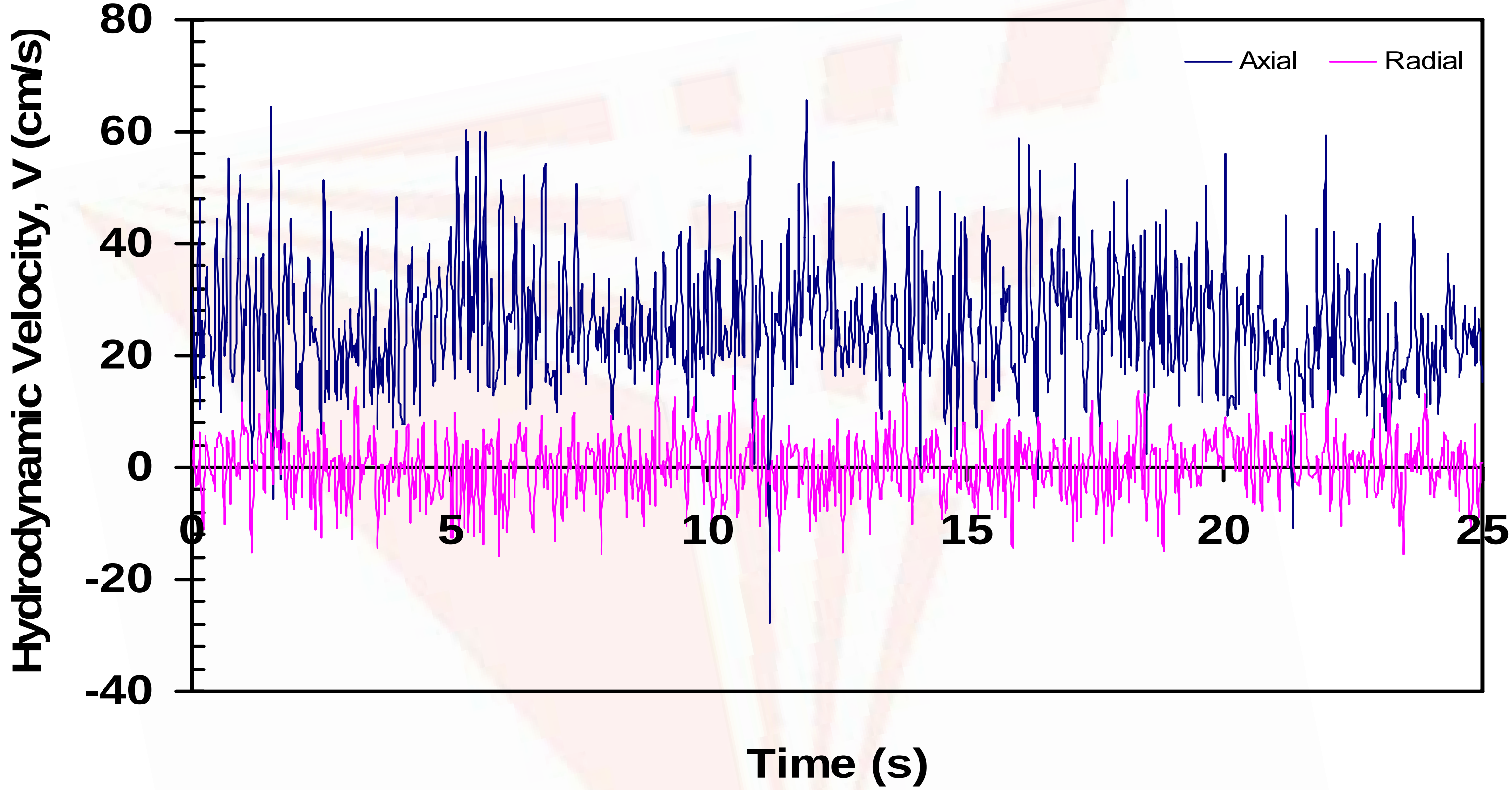

Oscillation of hydrodynamic velocity in radial and axial directions obtained by CCD camera technique at a measuring height 69.85 cm

$$(\overline{V_r} = 0.295 cm/s, \ \overline{V_a} = 25.68 cm/s)$$

ILLINOIS INSTITUTE OF TECHNOLOGY
Transforming Lives. Inventing the Future.

Laminar Normal Reynolds Stress

$$< C_i C_i > (r,t) = \frac{1}{n}\sum_{k=1}^{n}(c_{ik}(r,t) - v_i(r,t))(c_{ik}(r.t) - v_i(r,t))$$

Turbulent Normal Reynolds Stress

$$< V_i V_i > (r) = \frac{1}{m}\sum_{k=1}^{m}(v_{ik}(r,t) - \bar{v}_i(r))(v_{ik}(r,t) - \bar{v}_i(r))$$

where, **"n" is the number of particles per unit volume,**
"c" is instantaneous particle velocity in i-direction,
"v_i" is hydrodynamic velocity in i-direction,
"r" is any position,
"i" is x, y or z direction,
"m" is the total number of frames over a given time period
$\bar{v}_i$ **is the mean particle velocity**

Measured laminar and turbulent granular temperatures

(U_g = 46.67 cm/s, h = 69.85 cm)

Granular Temperature, m^2/s^2	
Laminar due to individual particle oscillations	**Turbulent due to cluster oscillations**
1.27×10^{-2}	6.73×10^{-3}

Laminar Granular Temperature

$$\theta_{Laminar}(r,t) = \frac{1}{3}\left[< C_x C_x > + < C_y C_y > + < C_z C_Z > \right]$$

$$\theta_{Laninar}\left(r,t\right) \cong \frac{1}{3}\left[2\left\langle C_x C_x \right\rangle + \left\langle C_y C_y \right\rangle\right]$$

Turbulent Granular Temperature

$$\theta_{Turbulent}(r,t) = \frac{1}{3}\left[< V_x V_x > + < V_y V_y > + < V_z V_Z > \right]$$

$$\theta_{Turbulent}\left(r,t\right) \cong \frac{1}{3}\left[2\left\langle V_x V_x \right\rangle + \left\langle V_y V_y \right\rangle\right]$$

Comparison of Granular Temperatures

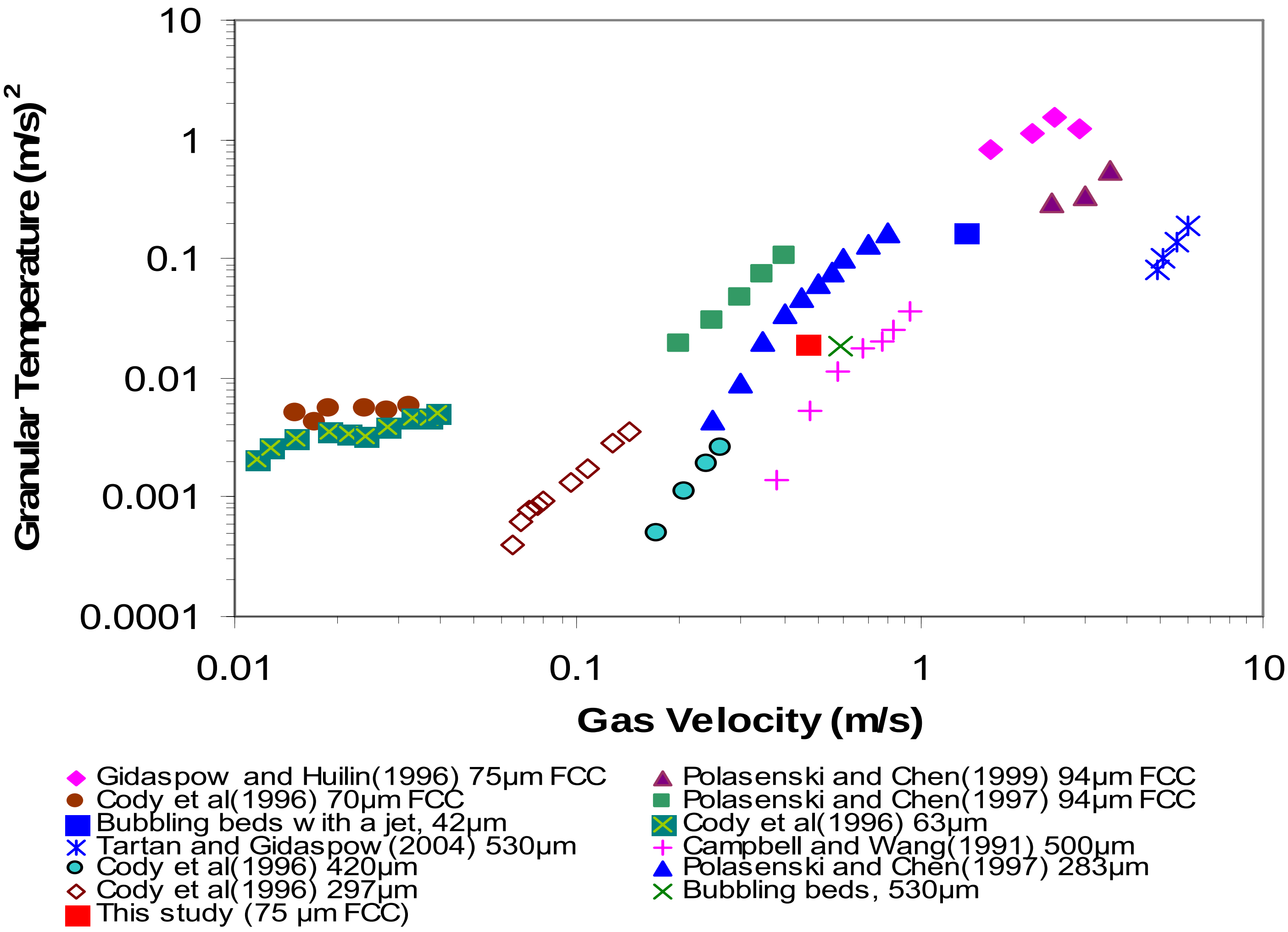

Measured axial and radial solids dispersion coefficients

(U_g = 46.67 cm/s, h = 69.85 cm)

Solids Dispersion Coefficient, m^2/s		
	Axial	Radial
Laminar	3.21×10^{-4}	7.66×10^{-5}
Turbulent	1.77×10^{-4}	3.78×10^{-5}

PART 5

Gasifier fuel cell

Hybrid gasification fuel cell-gas turbine-steam CC

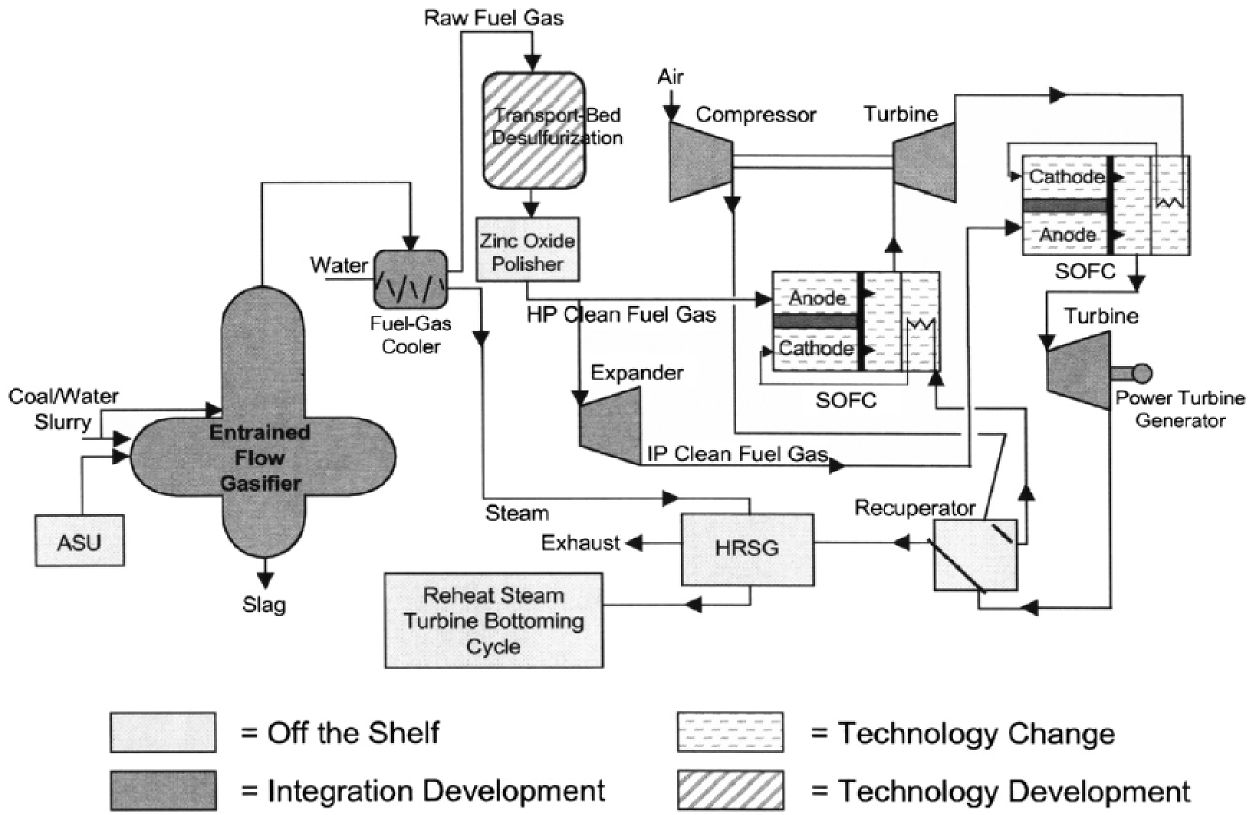

Department of Energy (DOE) vision 21 concept involves coal gasification with oxygen in an entrained flow gasifier and electricity production using solid oxide fuel cells and gas turbines. The use of oxygen to supply the heat necessary for the endothermic carbon – steam reaction requires an additional 34 % moles of carbon per mole of steam.

To improve this concept we combine the gasifier and the fuel cell into one unit in order to transfer heat from the fuel cell to the gasifier.

Ruth LA. US DOE Vision21 Workshop, FETC Pittsburgh,PA, Dec. 1998.

Ideal Gasifier Fuel Cell with Carbon Feed

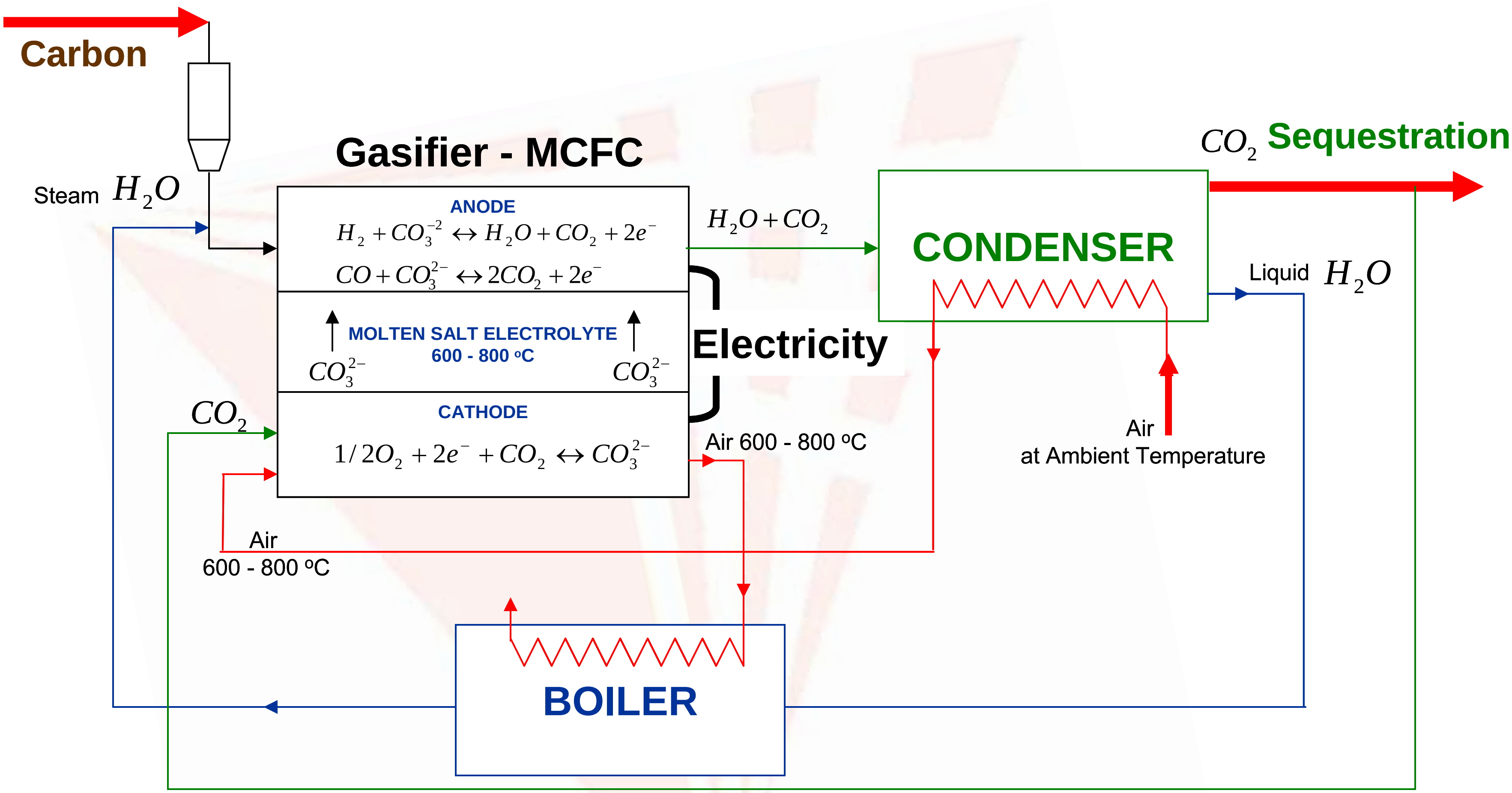

The overall reaction is as follows:

Gasification $\quad C + H_2O \rightarrow CO + H_2$

Fuel Cell $\quad CO + H_2 + O_{2,cathode} \rightarrow CO_2 + H_2O$

Net $\quad C + O_{2,cathode} \rightarrow CO_2$

Hence, ideally the gasifier fuel cell is 100% efficient, since $\Delta H = \Delta G =$ Electrical work

Coal Gasifier Fuel Cell System

ILLINOIS INSTITUTE OF TECHNOLOGY
Transforming Lives. Inventing the Future.

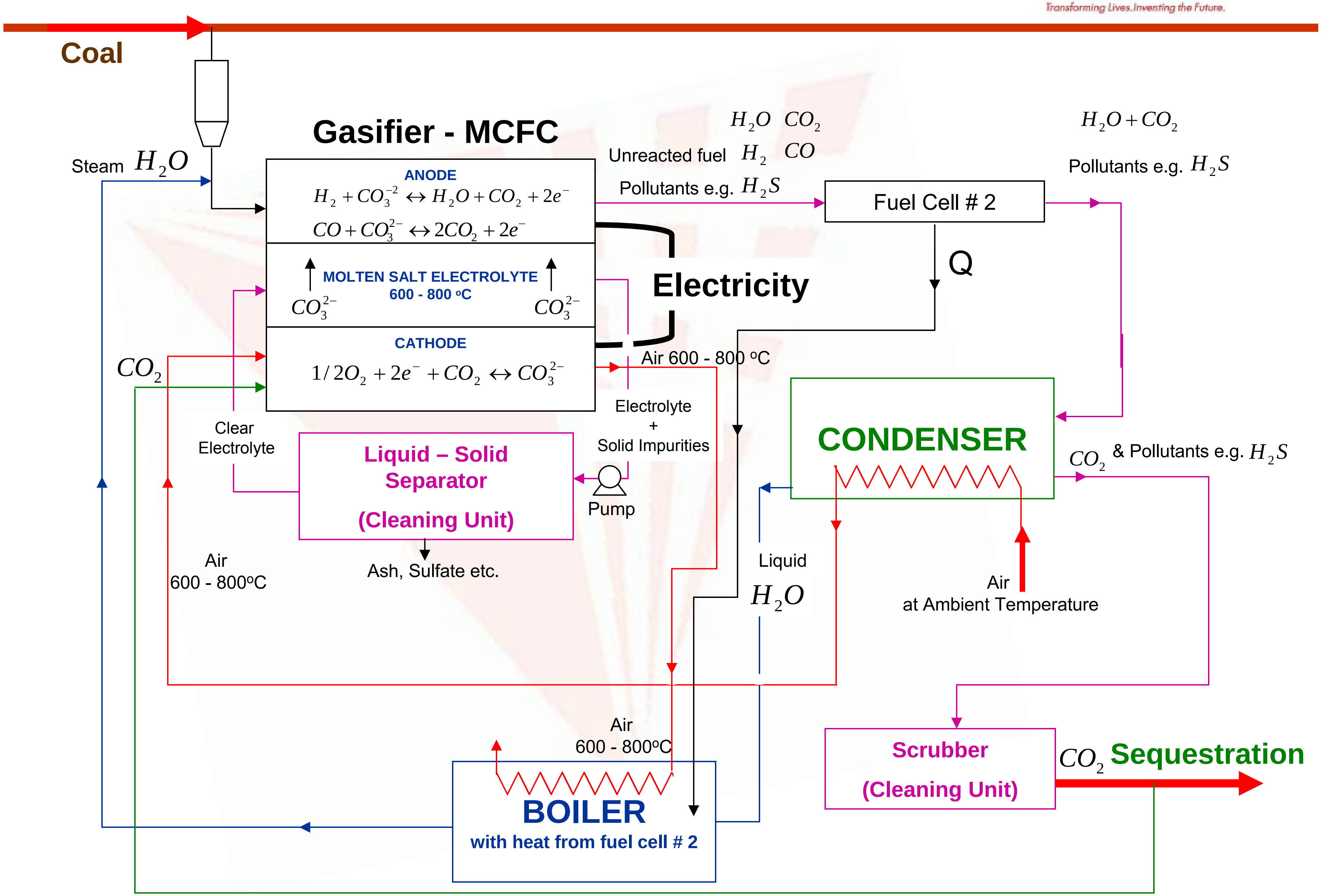

Kinetic Expression

Gasification reactions consist of 3 reactions as follows:

Reaction 1: $C + CO_2 \rightarrow 2CO$

Reaction 2: $C + 2H_2 \rightarrow CH_4$

Reaction 3: $C + H_2O \rightarrow CO + H_2$

Carbon particles react with components of the gas phase

In addition to the three heterogeneous reactions, the water gas shift reaction occurs in the gas phase

Water shift reaction $CO + H_2O \Leftrightarrow CO_2 + H_2$

Heterogeneous reaction model

The shrinking core model used to calculate the rate of the heterogeneous reactions is given by

$$R_i = \frac{\varepsilon_S\left(P_i - P_i^*\right)}{\dfrac{d_p}{6K_{p,i}} + \dfrac{d_p^2\left(1-\rho_{UC}\right)RT}{12\rho_{UC}D_{M,i}} + \dfrac{1}{\eta_i\rho_{UC}^3K_{r,i}C_C^0}}$$

Mass transfer **Diffusion** **Reaction**

Electrochemical Oxidation

ILLINOIS INSTITUTE OF TECHNOLOGY
Transforming Lives. Inventing the Future.

<u>Hydrogen System</u>

Anode $H_2 + CO_3^{-2} \leftrightarrow H_2O + CO_2 + 2e^-$

Cathode $1/2O_2 + 2e^- + CO_2 \leftrightarrow CO_3^{2-}$

Overall $H_2 + 1/2O_2 \leftrightarrow H_2O$

<u>Carbon monoxide System</u>

Anode $CO + CO_3^{2-} \leftrightarrow 2CO_2 + 2e^-$

Cathode $1/2O_2 + 2e^- + CO_2 \leftrightarrow CO_3^{2-}$

Overall $CO + 1/2O_2 \leftrightarrow CO_2$

Gasifier Fuel cell

The current density is given in Dharia (1977), in Gidaspow's report (1980,1984) and his book (1994) as

$$I_i = \left(E\left(P_i\right) - V_E\right) / R_{eff}$$

The reversible emf of fuel cell is obtained from the Nernst equation as a function of partial pressure.

$$E\left(P_{H_2}\right) = E_0 + \frac{RT}{2 \cdot F} \ln \frac{P_{H_2}^A \left(P_{O_2}^C\right)^{1/2}}{P_{H_2O}^A}$$

$$E\left(P_{H_2}\right) = E_0 + \frac{RT}{2 \cdot F} \ln \frac{P_{CO}^A \left(P_{O_2}^C\right)^{1/2}}{P_{CO_2}^A}$$

Rate consumption of hydrogen and carbon monoxide in a fuel cell is $\dfrac{I_i}{n_i F \alpha}$ **mol cm^{-3}s^{-1}**

where	I_i	-	**current density**	**A cm^{-2}**
	n_i	-	**2, number of electron produced per H_2 mole**	
			2, number of electron produced per CO mole	
	F	-	**96,500**	**C mol^{-1}**
	α	-	**2 mm, thickness of anode channel**	

Entire System Efficiency

The entire system efficiency is estimated from the output of electric power and the consumption of carbon in the batch system (Cordiner et al 2007)

$$\eta_g = \frac{P_{el}}{\dot{m}_{Carbon\ \ consumption} \Delta H_{C+O_2 \rightarrow CO_2}}$$

where P_{el} is the output electric power estimated by $P_{el} = V \iint I dx dy$ (Watt)

$\dot{m}_{Carbon\ \ consumption}$ is the rate of carbon consumption (g/s)

$\Delta H_{C+O_2 \rightarrow CO_2}$ is the heat formation of carbon dioxide (-29677 J/g)

Instantaneous Profiles

ILLINOIS INSTITUTE OF TECHNOLOGY
Transforming Lives. Inventing the Future.

for the hydrogen-carbon monoxide gasifier fuel cell, 1073 K, 0.6 V.

Solid Volume Fraction

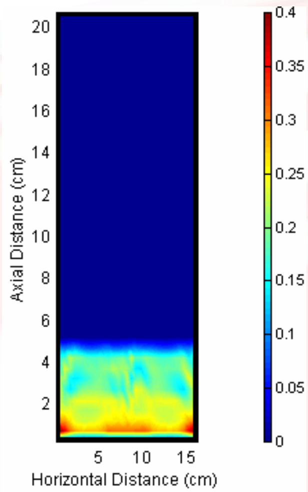

Weight Fraction of CO

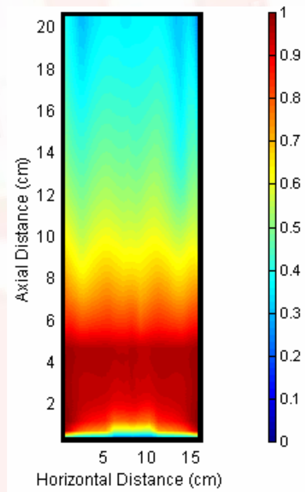

Weight Fraction of H_2

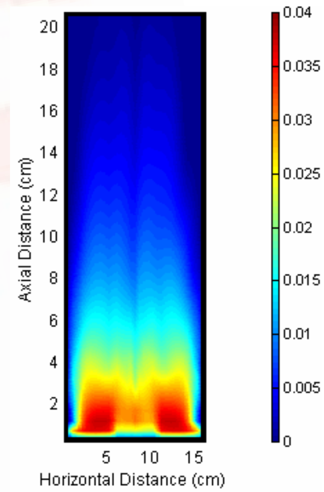

Gas Temperature (K)

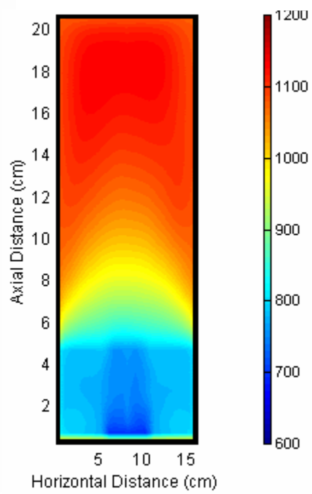

Current Density of CO

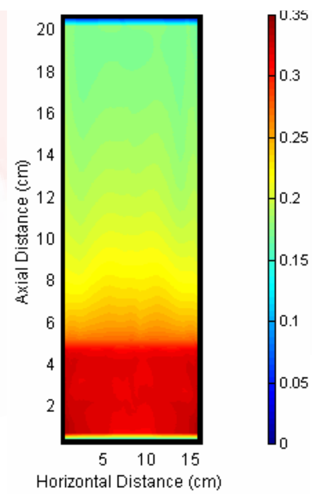

Current Density of H_2 (A/cm^2)

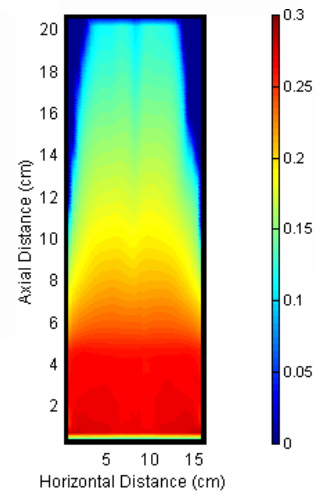

Axial Mole Fraction Profiles in Isothermal Gasifier

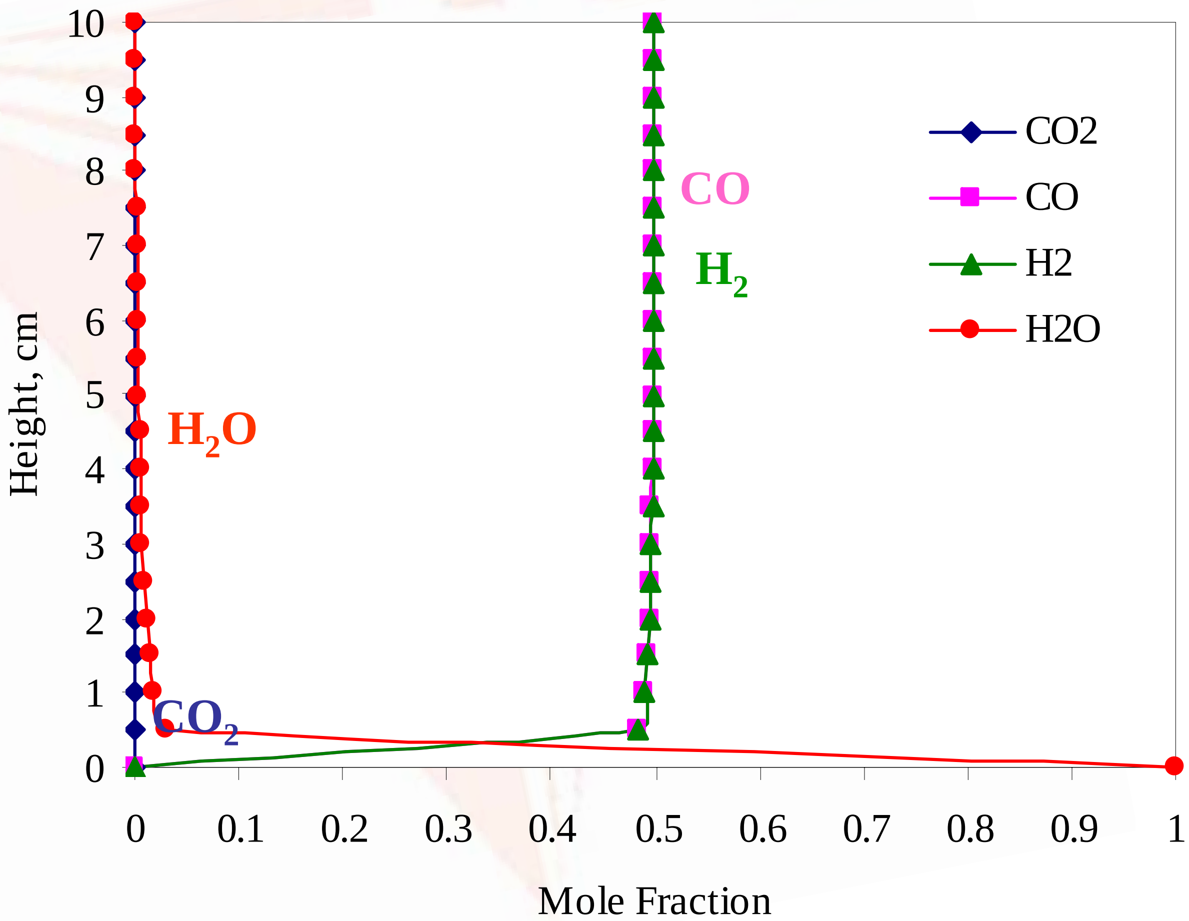

Isothermal gasification at 1073 K with the water gas shift reaction (b=100 in water gas shift equation) with inlet steam at a velocity of 7.3 cm/s

Axial mole fraction profiles in Gasifier Fuel Cell

The effect of the operating cell potential

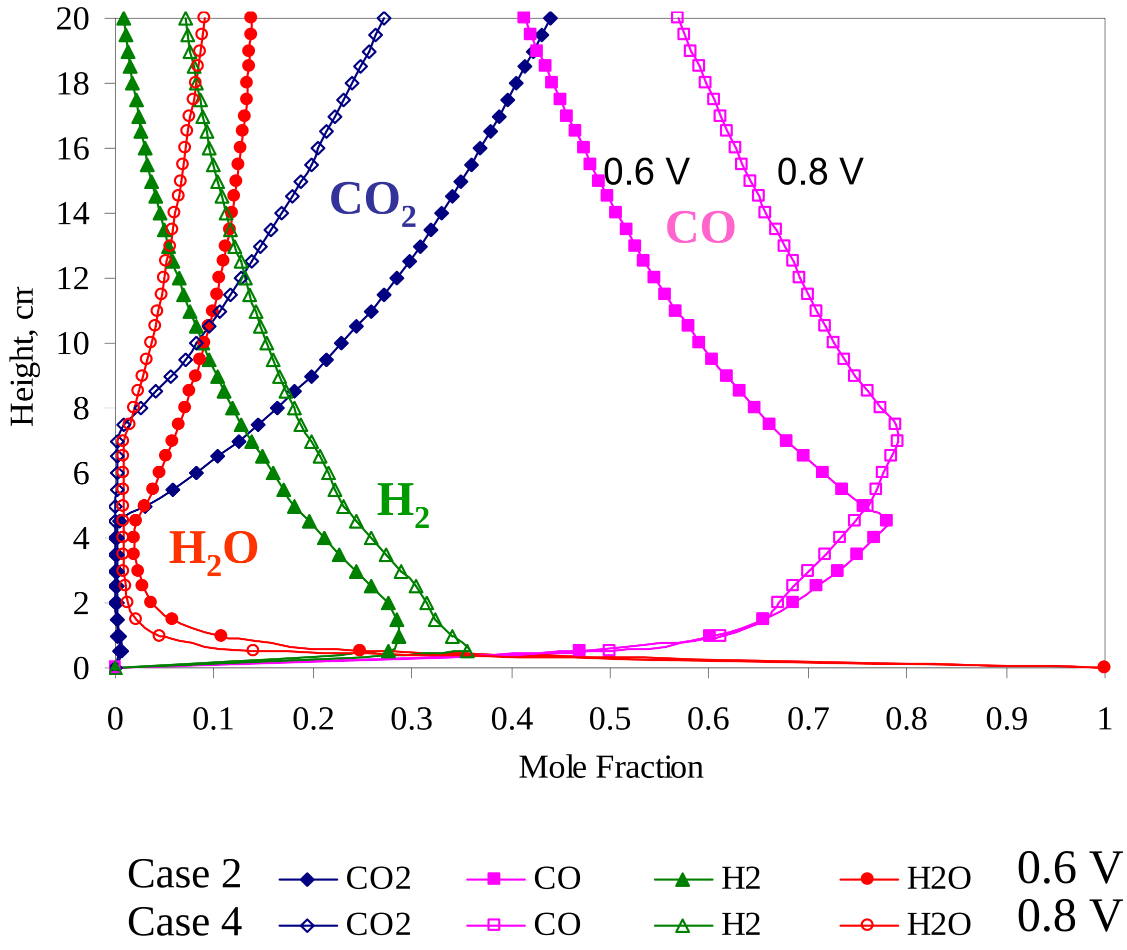

ILLINOIS INSTITUTE OF TECHNOLOGY
Transforming Lives. Inventing the Future.

Current Densities

of gasifier hydrogen and carbon monoxide fuel cells

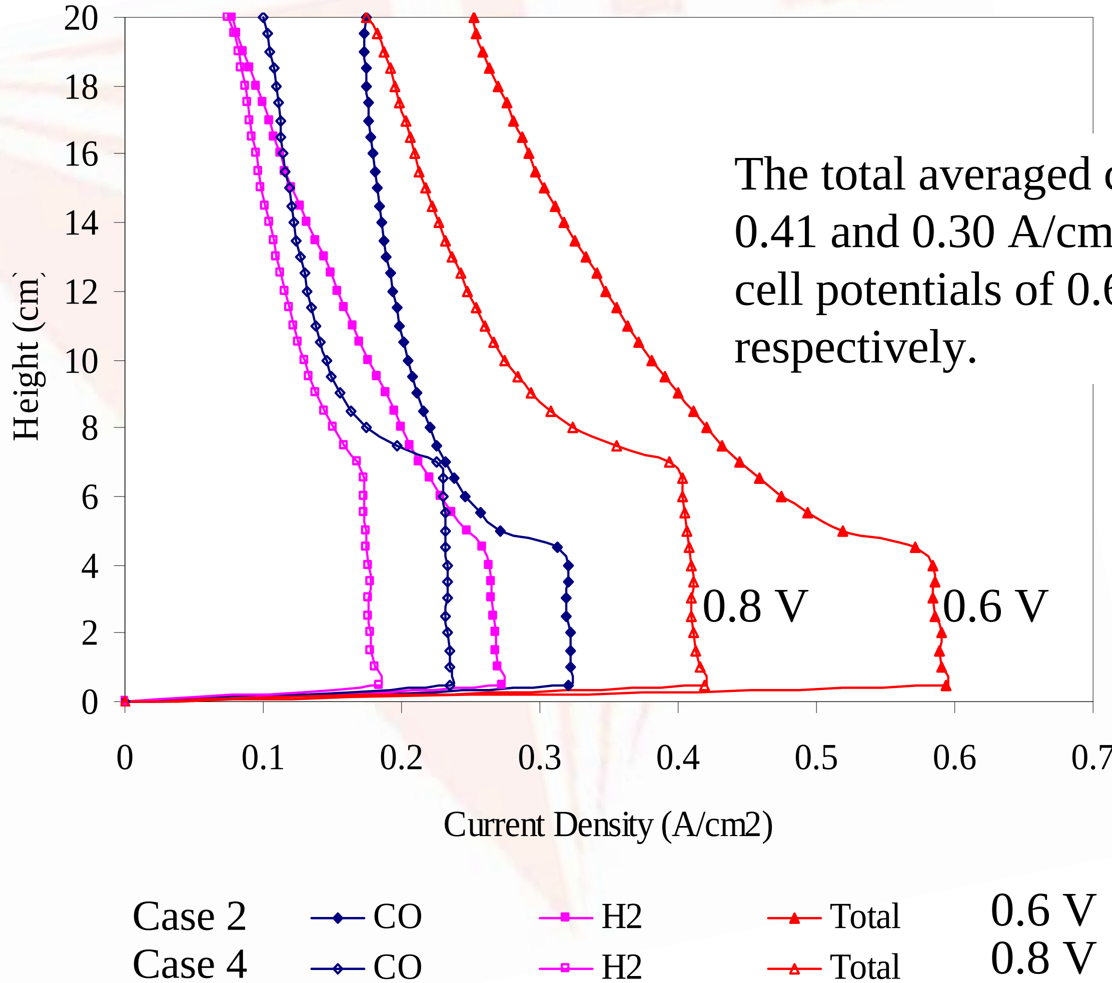

The total averaged current densities are 0.41 and 0.30 A/cm² based on operating cell potentials of 0.6 and 0.8 volts, respectively.

Weight Fraction of Carbon Conversion as a Function of Operating Time

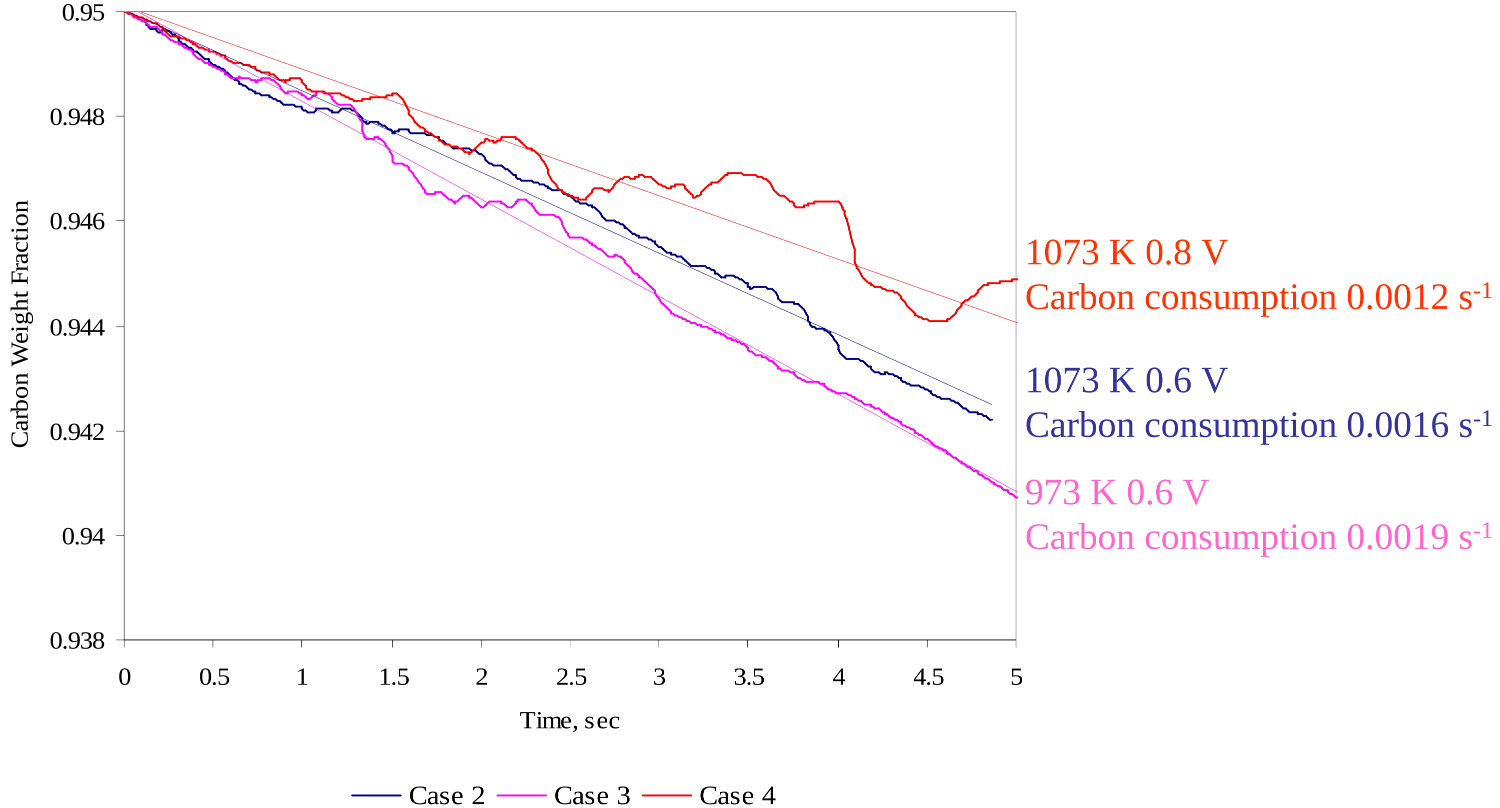

Case	**2**	**3**	**4**
Inlet steam temperature (K)	1073	973	1073
Operating cell potential (V)	0.6	0.6	0.8
The rates of carbon consumption (s^{-1})	0.0016	0.0019	0.0012

Gasifier Fuel Cell Efficiency

ILLINOIS INSTITUTE OF TECHNOLOGY
Transforming Lives. Inventing the Future.

The effect of the water gas shift reaction (cases 1 & 2)
The effect of the inlet steam temperature (cases 2 & 3)
The effect of the operating cell potential (cases 2 & 4)
The effect of the initial concentration of H_2O and CO_2 (cases 2 & 5)

Case	**1**	**2**	**3**	**4**	**5**
Parameter, b, in water gas shift	1	100	100	100	100
Inlet steam temperature (K)	1073	1073	973	1073	1073
Operating cell potential (V)	0.6	0.6	0.6	0.8	0.6
Initial weight fractions of H_2O and CO_2	0.5,0.5	0.5,0.5	0.5,0.5	0.5,0.5	0.05,0.05

Total Power (W)	72.96	96.41	101.84	93.44	95.85
Heat combustion (W)	158.21	140.62	193.71	157.72	140.7
Total Efficiency %	46.11	**68.56**	52.57	59.25	68.12

CONCLUSIONS
Gasifier fuel cell

ILLINOIS INSTITUTE OF TECHNOLOGY
Transforming Lives. Inventing the Future.

The new concept of the bubbling gasifier – fuel cell ideally allows

- **100% of carbon enthalpy conversion to electrical energy**
- **Formation of CO_2 as the only product ready for cleaning and sequestration**
- **High capacity storage of fuel: carbon, coal or biomass, not gases or liquid hydrogen**

However, optimization is required to get closer to 100% efficiency. The present scheme gives an efficiency of 68% and less.

SUMMARY

ILLINOIS INSTITUTE OF TECHNOLOGY
Transforming Lives. Inventing the Future.

Gasification Transport: A Multiphase CFD Approach and Measurements

- **We developed a new method for computing dispersion coefficients in risers and bubbling beds.**

  Jiradilok, V., D. Gidaspow, and R.W. Breault, "Computation of gas of solids dispersion coefficients in turbulent risers and bubbling beds," Article in press in Chemical Engineering Science, 2007 (www.sciencedirect.com)

  Jiradilok, V., D. Gidaspow, R.W. Breault, and L.J. Shadle, "Simulations of the NETL Morgantown riser cork data," submitted for publication

- **We developed a new PIV technique for measuring radial and axial dispersion coefficients in risers.**

- **We developed a more efficient coal gasifier system with CO_2 sequestration than that proposed for FutureGen.**

  Gidaspow D. and V. Jiradilok, "Nanoparticle gasifier fuel cell for sustainable energy future," Journal of Power Sources, **166** (2007) 400–410.

  Gidaspow D. and V. Jiradilok, "Efficient Coal Gasifier-Fuel Cell with CO2 Sequestration," The Clearwater Coal Conference, The 32nd International Technical Conference on Coal Utilization & Fuel Systems, Clearwater, Florida, U.S.A. June 13, 2007